

**2D SEISMIC REFLECTION DATA INTERPRETATION  
INTEGRATED WITH RESERVOIR CHARACTERIZATION  
OF MIANO AREA USING SEISMIC AND WELL LOG DATA**



**BY**

**NAVEED HAYAT KHAN**

**BS GEOPHYSICS 2013-2017**

**DEPARTMENT OF EARTH SCIENCES  
QUAID-I-AZAM UNIVERSITY ISLAMABAD**

**PAKISTAN**

**2017**

بِسْمِ اللَّهِ الرَّحْمَنِ الرَّحِيمِ

*In the name of Allah, the Most Merciful, the Most Kind*

## **CERTIFICATE**

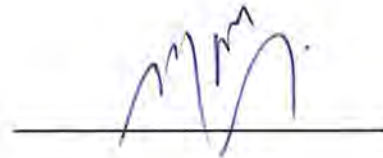
This dissertation is submitted by **NAVEED HAYAT KHAN S/O MUHAMMAD HAYAT KHAN** accepted in its present form by the Department of Earth Sciences, Quaid-i-Azam University Islamabad as satisfying the requirement for the award of BS degree in **Geophysics**.

### **RECOMMENDED BY**

**Mr ANEES BANGASH**  
(Supervisor)



**Dr. MONA LISA**  
(Chairperson,  
Department of Earth Sciences)



**EXTERNAL EXAMINER**



## DEDICATION

*My whole work is dedicated to my parents who have always loved me unconditionally and whose good examples have taught me to work hard for the things that I aspire to achieve.*

## ACKNOWLEDGEMENT

In the name of **Allah**, the most beneficent, the most merciful and all praises to Almighty Allah, the creator of this universe. I bear witness that there is no God but **Allah** and **Holy Prophet Hazrat Muhammad (P.B.U.H)** is the last messenger of **Allah**, whose life is a perfect model for the whole of mankind. All thanks to my **Allah**, who gave me the strength and ability to complete this project successfully. This thesis appears in its current form due to the assistance and guidance of several people. It gives me great pleasure to express my gratitude to all those who supported me and have contributed in making this thesis possible.

I express my profound sense of reverence to my supervisor **MR ANEES BANGASH**, Assistant Professor Department of Earth Sciences, Quaid-i-Azam University Islamabad who gave me the opportunity to work under his supervision. His continuous support, motivation and guidance have made this thesis possible. His vast knowledge and positive criticism motivated me to strive for the required results.

Good friends are like heaven on earth . I would like to express my appreciation to all of my friends and class fellows. At the end I specially acknowledge the prayers and efforts of my whole family, specially my parents and brothers for their encouragement, support and sacrifices throughout the study.

**NAVEED HAYAT KHAN**

## ABSTRACT

In this dissertation, focus is placed on the structural interpretation of the Miano block-20 in order to demarcate the probable zone for the accumulation of hydrocarbons. This thesis work includes preparation of synthetic seismogram of Miano-09 well. Analysis of geophysical borehole logs provides one of the best approaches to characterizing rocks within boreholes. So Facies analysis is also done in order to identify lithologies.

For the interpretation of the seismic lines, three reflectors are marked by correlating synthetic seismogram on seismic section. As the area of study lies in the Lower Indus Basin, horst and graben geometry in this region is common which is confirmed by fault polygon and time and depth contours made from time and depth grid respectively.

Facies modeling is one of the reliable tool for the confirmation of lithologies. In this dissertation, with the help of facies analysis of Miano-09 well, we came to the result revealing sand as the reservoir lithology.

Petrophysics is the one of the most reliable tools for the confirmation of the types of the hydrocarbon and for marking of the proper zone of the interest of the presence of the hydro carbon by combination of the different logs results. In this dissertation the petrophysics is performed on the Miano-09 and Miano-10 well and different zone of interest are marked where there is chance of the presence of the hydro carbon.



## Table of Contents

<b>CHAPTER 1</b> .....	<b>1</b>
1.1 Introduction to Study Area.....	1
1.2 Exploration History of Study Area .....	2
1.3 Objectives .....	2
1.4 Data used.....	3
1.4.1 Seismic Data .....	3
1.4.2 Well Data .....	4
1.5 Software used.....	6
1.6 Base Map .....	6
1.7 Workflow of Dissertation .....	7
<b>CHAPTER 2</b> .....	<b>9</b>
<b>GENERAL GEOLOGY AND STRATIGRAPHY OF THE AREA</b> .....	<b>9</b>
2.1 Introduction.....	9
2.2 Indus Basin.....	9
2.3 Tectonic and Stratigraphic Framework of Study Area .....	10
2.3.1 Central Indus Basin.....	11
2.3.2 Boundaries of Central Indus Basin .....	12
2.3.3 Geological Boundaries of Miano Area .....	12
2.4 Stratigraphy of the Study Area.....	13
2.5 Structure.....	13
2.6 Petroleum Play.....	13
2.6.1 Source Rock.....	14
2.6.2 Reservoir Rock.....	15
2.6.3 Seal Rock .....	15
2.6.4 Traps .....	15
<b>CHAPTER 3</b> .....	<b>16</b>
<b>SEISMIC INTERPRETATION</b> .....	<b>16</b>
3.1 Seismic Methods.....	16
3.1.2 Seismic Reflection Method.....	16

3.2 Seismic Interpretation .....	16
3.3 Workflow for Seismic Interpretation .....	17
3.4 Fault Marking.....	17
3.5 Horizon Picking .....	18
3.6 Interpreted Seismic Sections.....	18
3.7 Generation of Synthetic Seismogram .....	22
3.8 Generation of Fault Polygon.....	24
3.9 Contour Map.....	25
3.9.1 Time Contour Map.....	25
3.9.2 Depth Contour Map .....	27
<b>CHAPTER 4.....</b>	<b>29</b>
<b>SEISMIC ATTRIBUTES.....</b>	<b>29</b>
4.1 Introduction.....	29
4.2 Physical Attributes.....	29
4.3 Geometrical Attributes.....	29
4.4 Envelope of Trace on Line P2094-223 .....	29
4.5 Instantaneous Frequency.....	30
4.6 Instantaneous Phase .....	31
<b>CHAPTER 5.....</b>	<b>33</b>
<b>PETROPHYSICAL ANALYSIS.....</b>	<b>33</b>
5.1 Introduction.....	33
5.2 Petrophysics .....	33
5.3 Raw Log Curve.....	33
5.3.1 Lithology Track.....	34
5.3.2 Resistivity Track.....	34
5.3.3 Porosity Track.....	35
5.4 Work Flow for Petrophysical Interpretation .....	35
5.5 Calculating Rock Properties of wells Miano-9 and Miano-10.....	36
5.5.1 Volume of Shale.....	37
5.5.2 Porosity Calculation.....	37
5.5.3 Water Saturation (Sw).....	39
5.5.4 Hydrocarbon saturation ( $S_h$ ).....	42



<b>1.1 5.6 Well Interpretation of Miano-9</b>	<b>42</b>
5.7 Well Interpretation of Miano-10.....	43
<b>Chapter 06 .....</b>	<b>45</b>
<b>Rock Physics .....</b>	<b>45</b>
6.1 Estimation of Rock Physics .....	45
6.2 Seismic Waves and Elastic Modulli.....	46
6.2.1 Shear Modulus .....	46
6.2.3 Young's Modulus.....	46
6.2.4 Poisson Ratio .....	47
6.3 Rock Properties of Miano-9.....	47
<b>CHAPTER 7.....</b>	<b>49</b>
<b>FACIES ANALYSIS.....</b>	<b>49</b>
7.1 Introduction.....	49
7.2 Walther's Law of Facies .....	50
7.3 Facies Analysis .....	50
7.3.1 Procedure of Facies Analysis.....	51
7.3.2 Facies Analysis of Well Miano-9.....	51
<b>Discussions and Conclusions.....</b>	<b>54</b>
<b>References.....</b>	<b>55</b>

## **List of Figures**

- Figure 1.1 Location of study area (Miano) (Google Earth)
- Figure 1.2 Geological boundaries of study area (Raza et al., 1989).
- Figure 1.3 Base map of study area with highlighted lines
- Figure 1.4 Workflow of Dissertation
- Figure 2.1 Tectonic Map of Pakistan (Kazmi and Rana, 1982)
- Figure 2.3 Regional tectonic framework of Miano Field within Central Indus Basin (Mehmood et al., 2004).
- Figure 2.4 Boundaries of Central Indus Basin.
- Figure 2.5 Tectonic boundaries of Miano Block-20.
- Figure 2.6 Stratigraphic column of study area (Mehmood et al., 2004)
- Figure 3.1 Work Flow of seismic interpretation.
- Figure 3.2 Interpretated time section of P2094-223.
- Figure 3.3 Depth section of line P2094-223.
- Figure 3.4 Interpreted time section of line P2094-219.
- Figure 3.5 Depth section of line P204-219.
- Figure 3.6 Interpreted strike line (P2094-214).
- Figure 3.7 Interpreted strike line (P2094-216).
- Figure 3.8 Process of convolution and making of synthetic seismogram (Courtesy IHS).
- Figure 3.9 Synthetic Seismogram of Miano-9.
- Figure 3.10 Correlating Synthetic with Seismic line P2094-223
- Figure 3.11 Fault polygon of B-interval.

Figure 3.12 Time contour Map of B-interval.

Figure 3.13 Depth contour map of B-interval.

Figure 4.1 Envelope Attribute on line P2094-223.

Figure 4.2 Instantaneous Frequency calculated for seismic line P2094-223.

Figure 4.3 Instantaneous Phase calculated for line P2094-223.

Figure 5.1 Basic three log Tracks.

Figure 5.2 Work flow for petro physical analysis.

Figure 5.3 Workflow for calculating  $R_w$ .

Figure 5.4 Schlumberger chart showing value of  $R_{meq}$ .

Figure 5.5 (a) Calculated value of  $R_{meq}$  Sp Chart-1. (b) Calculated value of  $R_w$ .

Figure 5.6 Petrophysical analysis of Miano-9.

Figure 5.7 Petro physical analysis of Miano-10

Figure 6.1 Work flow for calculating rock properties.

Figure 6.3 Behavior of rock properties calculated for well Miano-9.

Figure 7.1 Major depositional environments ( Rais et al., 2012).

Figure 7.2 Depositional setting purposed by walther.

Figure 7.3 Workflow for Facies analysis.

Figure 7.4 Facies analysis between DTCO and NPHI.

Figure 7.5 Facies analysis between NPHI and RHOB.

## CHAPTER 1

### 1.1 Introduction to Study Area

The Miano gas field is located in the Thar Desert 62 km southeast of Sukkur, Pakistan and its length along strike is nearly 42km. It is thought to extend from the southern block boundary in a north-northeasterly direction and it lies north of the Kadanwari gas field. The study area is bounded by latitudes  $27^{\circ} 14' N$  to  $27^{\circ} 32' N$  and longitudes  $69^{\circ} 12' E$  to  $69^{\circ} 28' E$  and is a part of the Block 20, which lies in the northern part of lower Indus basin (central Indus basin). A satellite image of Pakistan is given in Figure 1.1 showing the Miano block (Khan et al., 2008). The survey was carried out by OMV in 1994. The purpose of the study was to locate the prospective. Geological boundaries and location of Miano area is shown in Figure 1.2.



Figure 1.1 Location of study area (Miano) (Google Earth).

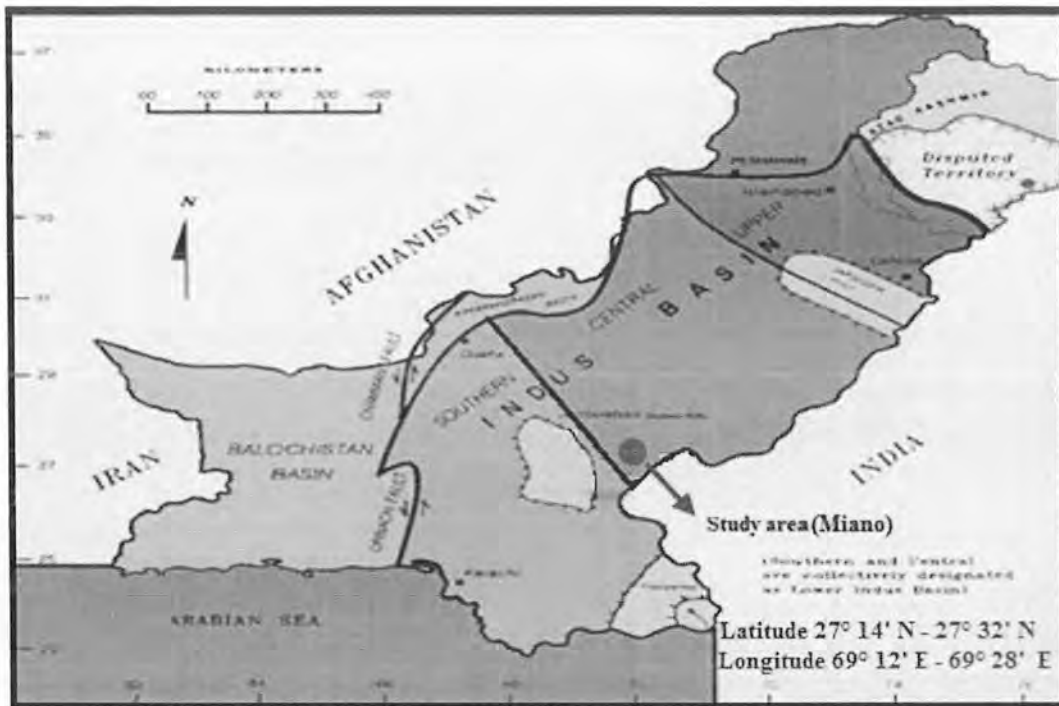


Figure 1.2 Geological boundaries of study area (Raza et al., 1989).

## 1.2 Exploration History of Study Area

Miano gas field is located in Sindh Province. It is a joint venture between OMV Exploration (Pakistan), ENI Exploration and Production Limited (Italy), Pakistan Petroleum Limited (PPL) and Oil and Gas Development Company Limited (OGDCL). To appraise the Miano field targeting the lower Cretaceous aged Lower Goru formation total eighteen wells have been drilled out of which only seven wells are currently on production (PPL). Miano raw gas is being processed at Kadanwari gas processing plant, which has been upgraded. The average gas sales from Miano field are 145 MMSCFD. Currently seven wells are on production and an average gas sale is around 145 MMSCFD. The average daily sale during 2004-05 (up to May 2005) from the field was 141.22 MMSCFD of purified gas, and 104 barrels of condensate (Pakistan petroleum Limited).

## 1.3 Objectives

The main objectives of this dissertation based on interpretation of seismic section are:

- Detailed seismic structural interpretation for identification of structures favorable for hydrocarbon accumulation.

- Seismic attribute analysis provides some qualitative information of the geometry and confirms the seismic interpretation.
- Identification of the possible hydrocarbons bearing zones by means of Petrophysical analysis by using available well data.
- Facies analysis helps in identifying the lithologies of the reservoir zone.

## 1.4 Data used

Data used for this dissertation:

- Seismic data in SEG-Y format
- LAS file(well log data)
- Navigation file

### 1.4.1 Seismic Data

The data used for current research includes 11 seismic lines and three wells Miano-7, Miano-9 and Miano-10. The orientation of Seismic lines and the wells are listed in the table 1.1. Four lines and two wells (in bold) are assigned to me for the completion of this research work.

Table 1.1 Data used for research work

SR.NO.	LINE	OREINTATION	SHOT POINTS	NATURE	WELL
1	P2094-211	N-S	102-739	DIP	MIANO-9
2	P2094-212	E-W	102-500	STRIKE	<b>MIANO-10</b>
3	P2094-213	N-S	102-740	DIP	
4	<b>P2094-214</b>	<b>E-W</b>	<b>102-1175</b>	<b>STRIKE</b>	
5	P2094-215	N-S	103-852	DIP	
6	<b>P2094-216</b>	<b>N-S</b>	<b>103-852</b>	<b>STRIKE</b>	
7	P2094-217	N-S	102-916	DIP	

8	P2094-219	N-S	102-1140	DIP
9	P2094-220	E-W	102-785	STRIKE
10	P2094-221	N-S	102-1142	DIP
11	P2094-223	N-S	102-1153	DIP

### 1.4.2 Well Data

Information about the well used in this research is given below in table 1.2 and 1.3.

**Table 1.2 Well data of Miano-9**

<b>WELL</b>	MIANO-9
<b>LATITUDE</b>	027.371747
<b>LONGITUDE</b>	069.311478
<b>KB</b>	80.00
<b>TOTAL DEPTH</b>	3385.0000(m)
<b>STATUS</b>	DEVELOPMENT
<b>EXPLORATION</b>	GAS
<b>SOURCE</b>	VIBROSEIS
<b>COMPANY</b>	OMV(PAK.)
<b>FORMATION TOPS</b>	<b>DEPTH(m)</b>
Siwalik	000000.0
Kirthar Formation	000497.0
Drazinda Member	000497.0
Pirkoh Member	000572.0
Habib Rahi Member	000742.0
Ghazij Member	000871.0
Laki	000871.0
Sui Main Limestone Member	001512.0
Ranikot Formation	001697.0
Phar Formation	001860.0

Upper Goru	001930.0
Goru	001930.0
Shale Unit	002261.0
Lower Goru	002261.0
D Interval	003089.0
C Interval	003167.0
B Interval	003331.0

**Table 1.3 Well data of Miano-10**

<b>WELL</b>	<b>MIANO-10</b>
<b>LATITUDE</b>	<b>027.392528</b>
<b>LONGITUDE</b>	<b>069.31338</b>
<b>KB</b>	<b>77.0000</b>
<b>TOTAL DEPTH</b>	<b>3610.0000 (m)</b>
<b>STATUS</b>	<b>DEVELOPMENT</b>
<b>EXPLORATION</b>	<b>GAS</b>
<b>SOURCE</b>	<b>VIBROSEIS</b>
<b>COMPANY</b>	<b>OMV(PAK.)</b>
<b>FORMATION TOPS</b>	<b>DEPTH(m)</b>
Siwalik	000000.0
Kirthar Formation	000492.0
Pirkoh Member	000562.0
Habib Rahi Member	000742.0
Laki	000669.0
Sui Main Limestone Member	001490.0
Ranikot Formation	001673.0
Phar Formation	001822.0
Upper Goru	001918.0



Lower Goru	002256.0
Shale Unit	002256.0
D Interval	003072.0
C Interval	003149.0
B Interval	003317.0
A Interval	003506.0

### 1.5 Software used

Software's used in this research are;

- IHS Kingdom
- Matlab 2013
- Microsoft Office
- Snagit Editor

### 1.6 Base Map

Base map usually shows the seismic lines orientations, wells locations and seismic shot points along with the concession boundaries (Sroor, 2010) as shown in Figure 1.3. Four Lines i.e. two strikes P2094-214, P2094-216, two dip lines P2094-219 and P2094.223 and two wells Miano-9, Miano-10 are assigned to me. In Figure 1.3 Base map is shown with Highlighted lines which are assigned to me for this research work.

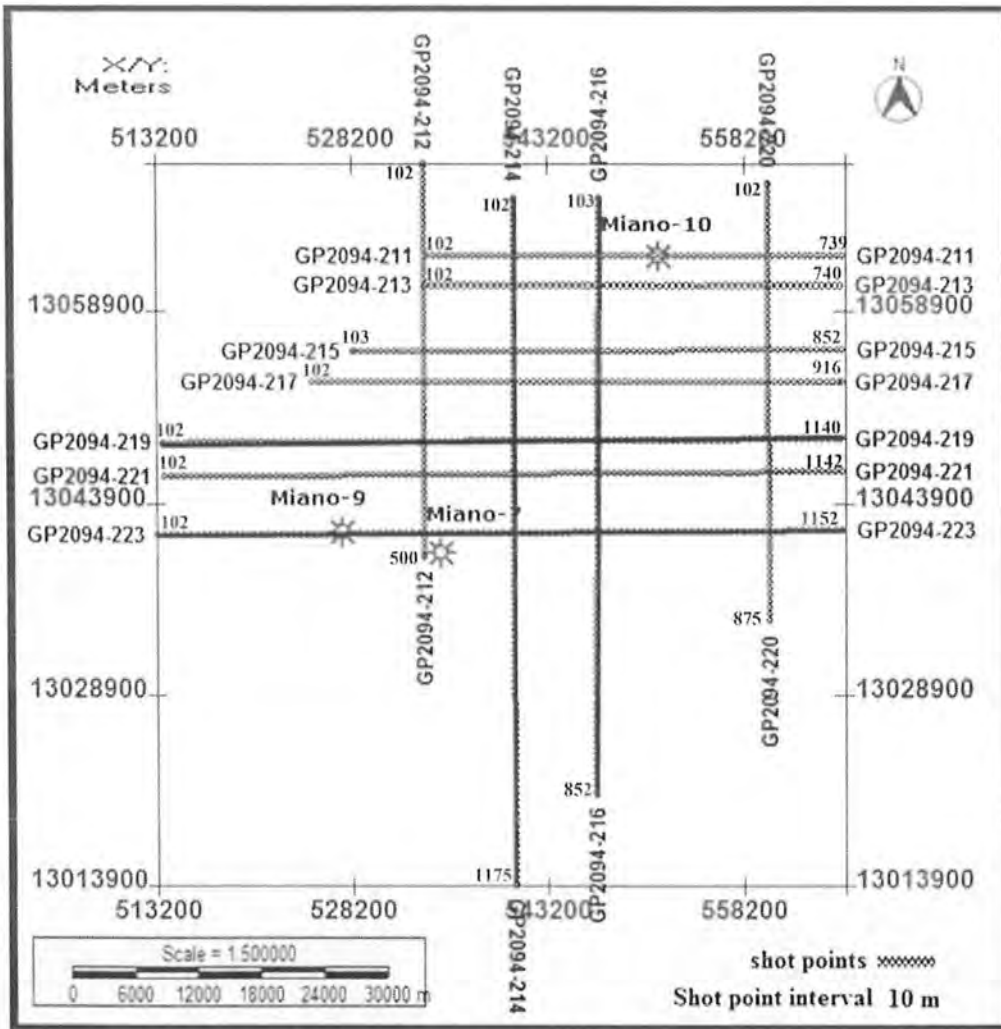


Figure 1.3 Base map of study area with highlighted lines.

## 1.7 Workflow of Dissertation

Base map is prepared by loading seismic data in SEG-Y format and navigation data in (X,Y) horizons and faults identify in seismic section to generate fault polygon and grid of marked horizons then two way time contour map and depth contour map are generated, Petrophysical analysis, Estimation of rock properties of reservoir and Facies analysis are performed by using well log data and AVO modeling as shown in Figure 1.4.

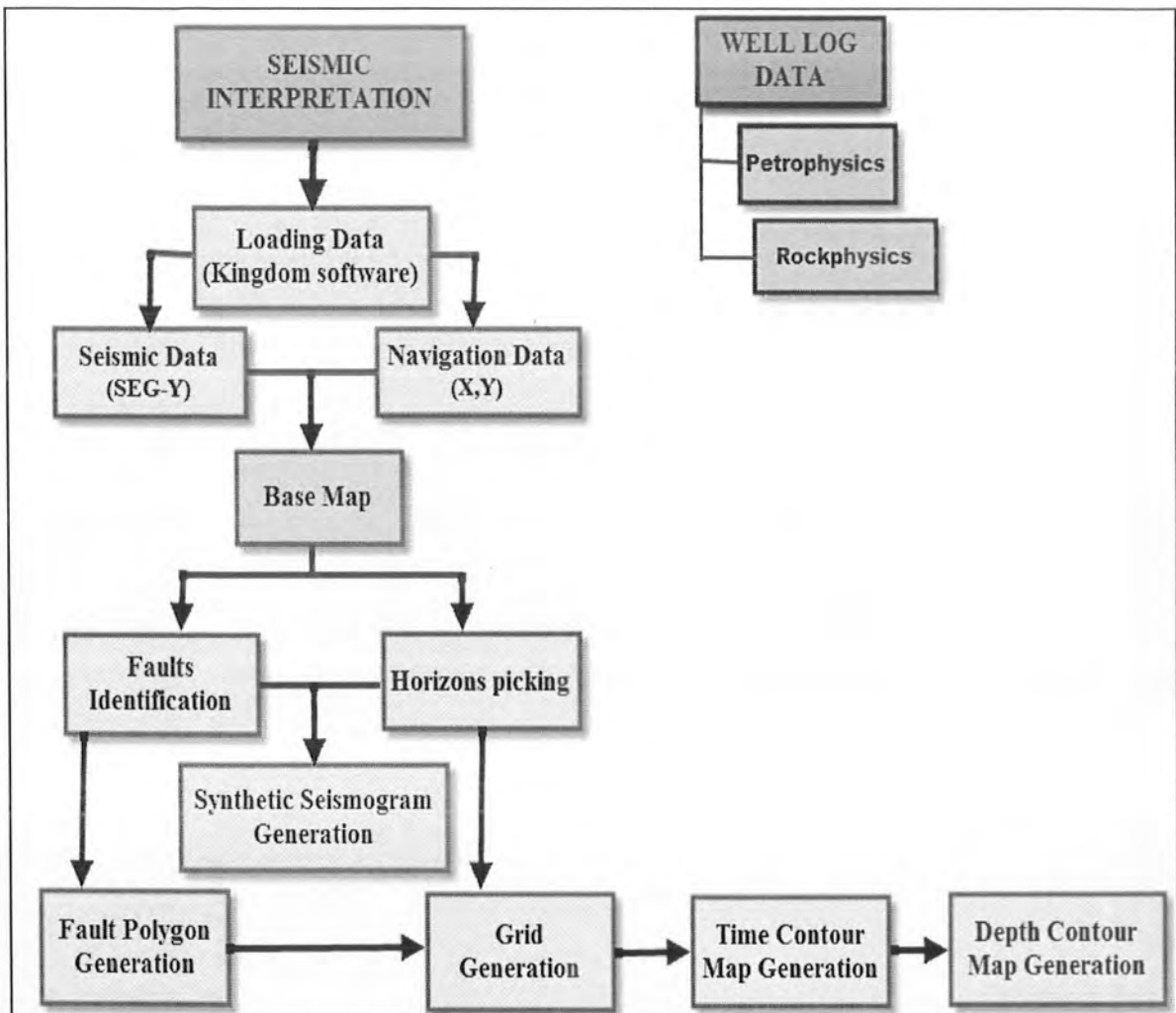


Figure 1.4 Workflow of Dissertation.

## CHAPTER 2

### GENERAL GEOLOGY AND STRATIGRAPHY OF THE AREA

#### 2.1 Introduction

Geology is the science comprising the study of solid Earth, the rocks of which it is composed, and the processes by which it evolves. In modern times for exploration of hydrocarbon general geology and geological history plays a very important role (Kazmi and Jan, 1997).

For seismic interpretation, it is necessary to know about the geology of the area, because same velocity effects can be generated from formations of different lithology. In order to deal with such complexities an interpreter must have background knowledge of geology about the area (Kazmi & Jan, 1997). Study area is located at the boundary of central or southern Indus basin collectively called Lower Indus basin. From Permian through middle Jurassic time, the area known today as Indus Basin is located in the southern hemisphere. Pakistan is unique as it lies at the junction of two convergent Indian and Eurasian plate (Kazmi & Jan, 1997). Due to the plate movement, tectonic features and structure, Pakistan is divided into following tectonic zones that are shown in Figure 2.1. This chapter deals with a brief description of the tectonics and structural setting. The hydrocarbon significance of the area is also incorporated in this chapter.

#### 2.2 Indus Basin

Indus basin is divided into Compression regime in upper Indus basin, Basement uplift in central Indus basin and Extensional regime in lower Indus basin. Tectonically Indus basin is much stable area as compared to other tectonic zones of Pakistan (Kazmi and Jan, 1997).

- Upper Indus Basin (North)
- Lower Indus Basin (South)

Further division of Indus Basin is shown below in Figure 2.2.

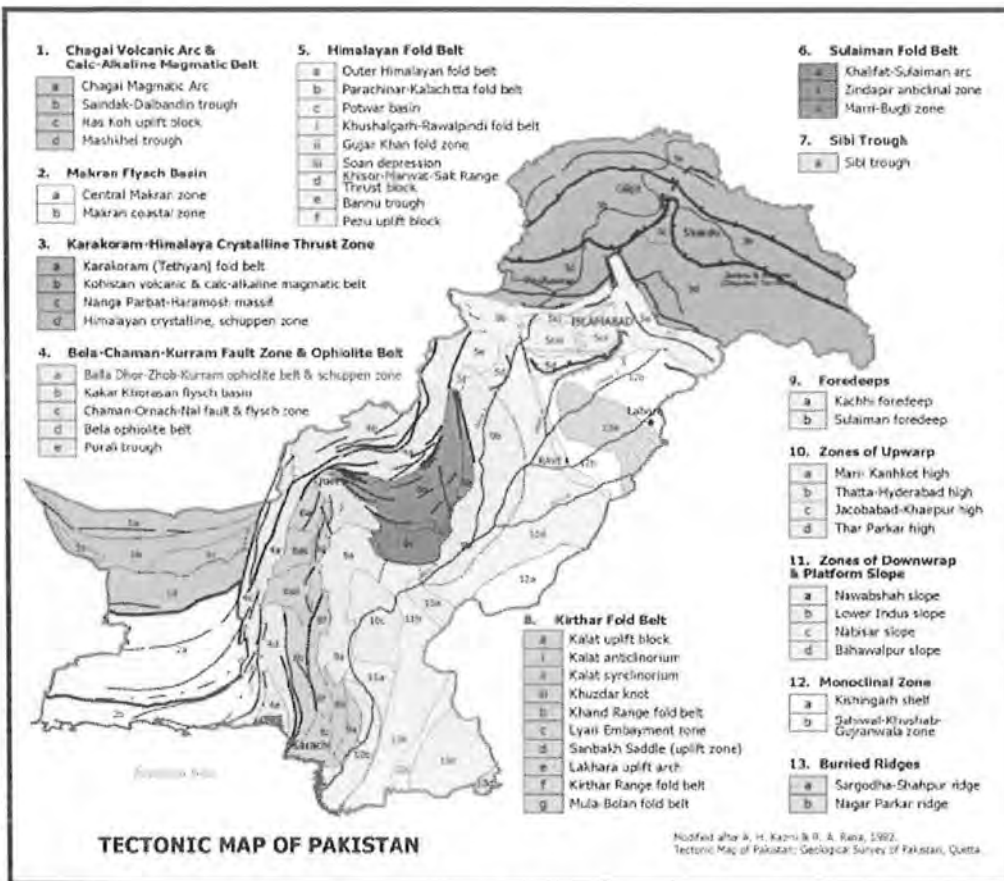


Figure 2.1 Tectonic Map of Pakistan (Kazmi and Rana, 1982)

## 2.3 Tectonic and Stratigraphic Framework of Study Area

Miano field is located in Sindh Province on the southeastern flank of a regional high, called Jacobabad-Khairpur High (Figure 2.3) approximately 62km southeast of Sukkur, Pakistan in Central Indus Basin and the length of the field along strike is nearly 42km. The study area lies at the boundary of Central Indus Basin. The uplift episode occurred near cretaceous-tertiary (K-T) boundary established as the base of Tertiary unconformity against which many of the deep basement related and shallower wrench-tectonics related faults terminate. Indus basin covers an area of about 533,500 sq. km (Kazmi and Jan, 1997).

### 2.3.1 Central Indus Basin

Central Indus basin is located in south of Sukkur Rift which divides the Lower Indus basin into Central and Southern Indus basin. Area is bounded by Marginal zone of Indian plate in west, Sukkur Rift in south and in East Indian Shield is present shown in Figure 2.3.

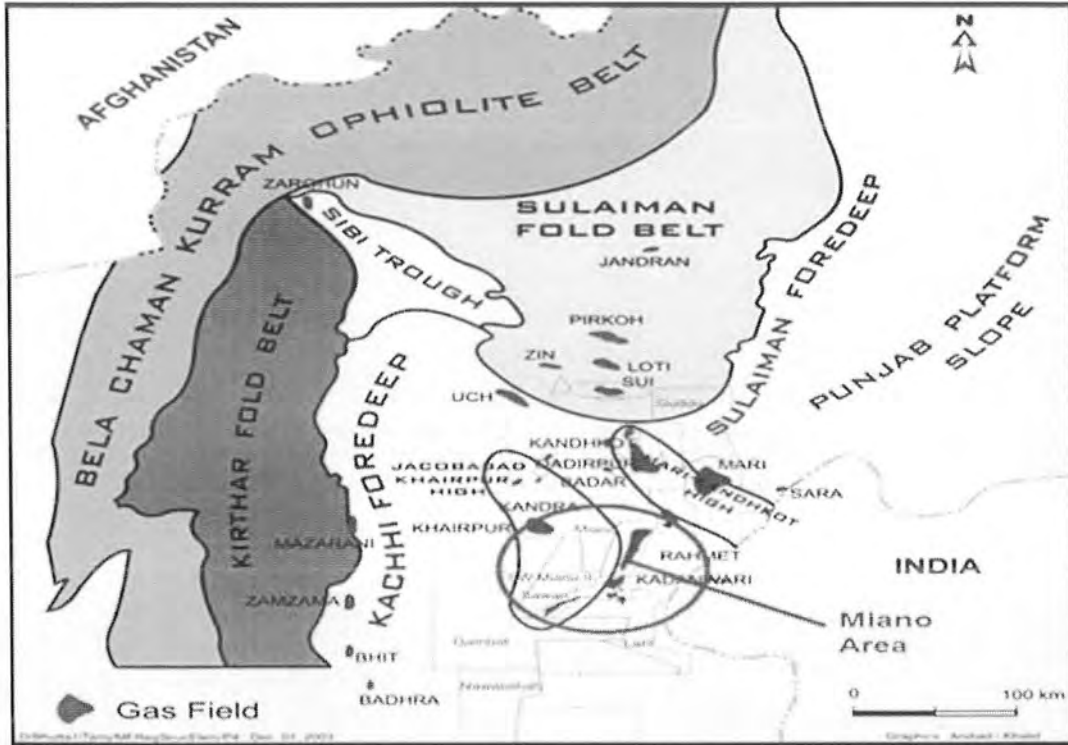


Figure: 2.3 Regional tectonic framework of Miano Field within Central Indus Basin (Mehmood et al., 2004).

### 2.3.2 Boundaries of Central Indus Basin

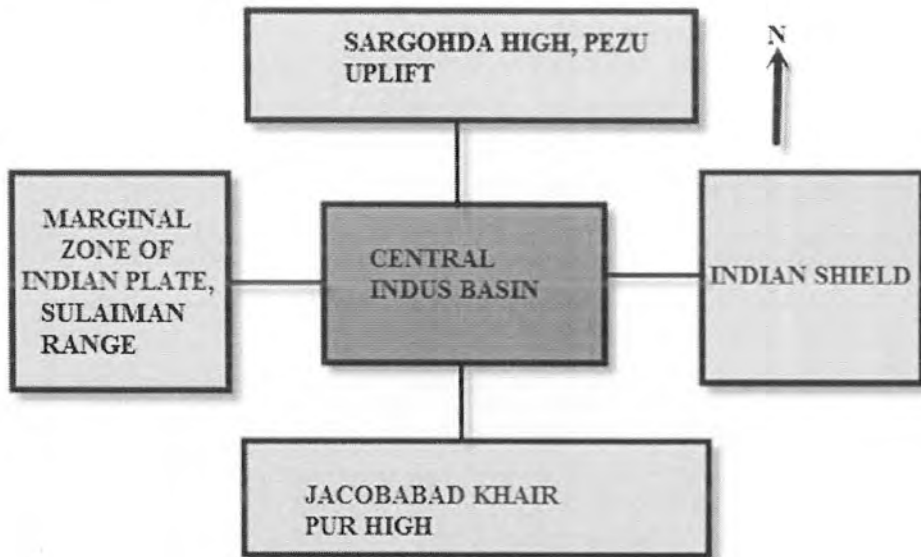


Figure 2.4 Boundaries of Central Indus Basin.

### 2.3.3 Geological Boundaries of Miano Area

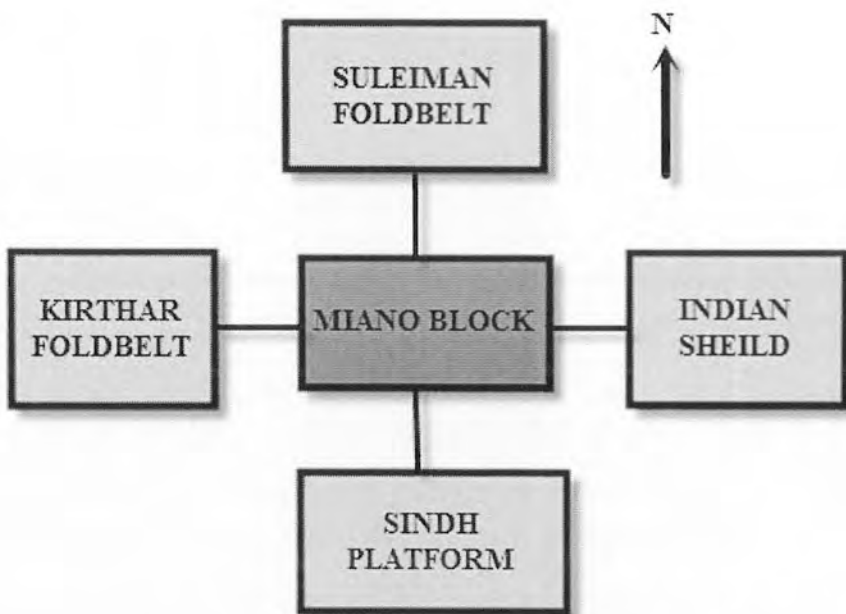


Figure 2.5 Tectonic boundaries of Miano Block-20.

## 2.4 Stratigraphy of the Study Area

The sedimentary section of the study area lies in central Indus basin mainly comprises of Permian to Mesozoic rocks and overlying by strong angular unconformity of late Paleozoic age. The Mesozoic progradational sequence is deposited on eastward inclined gentle slope. In the Thar slope areas all of Mesozoic sediments are regionally plunging towards the west and are truncated unconformably by volcanic rocks (basalts of Khadro formation). Permian, Triassic and early Jurassic sedimentary rocks in the study area consists of inter-bedded sandstone, siltstone and shale of continental to shallow marine origin. The sedimentary cover in the study area consists mainly of Permian to Mesozoic sedimentary rocks (Kadri, 1994). Stratigraphic chart of study area is shown in Figure 2.6.

## 2.5 Structure

Structural basement comprises thick Chiltan Formation of Middle and Upper Jurassic age. Miano field (study area) lies in extensional regime usually show normal faulting in NNW-SSE direction. Structure formed in the study area is Horst and Graben in nature.

## 2.6 Petroleum Play

In geology a petroleum play is a group of oil fields or prospects present in the same region that are controlled by the same set of geological circumstances (Stoneley, 1995). Lower Indus is the main hydrocarbons producing basin of the Pakistan 37% hydrocarbons of the Pakistan are extract from the lower Indus basin (Kadri, 1995). Within a basin the presence of play elements plays important role in hydrocarbon accumulation.

- Mature Source rock
- Migration pathway
- Reservoir rock
- Trap
- Seal or Cap rock
- Appropriate timing



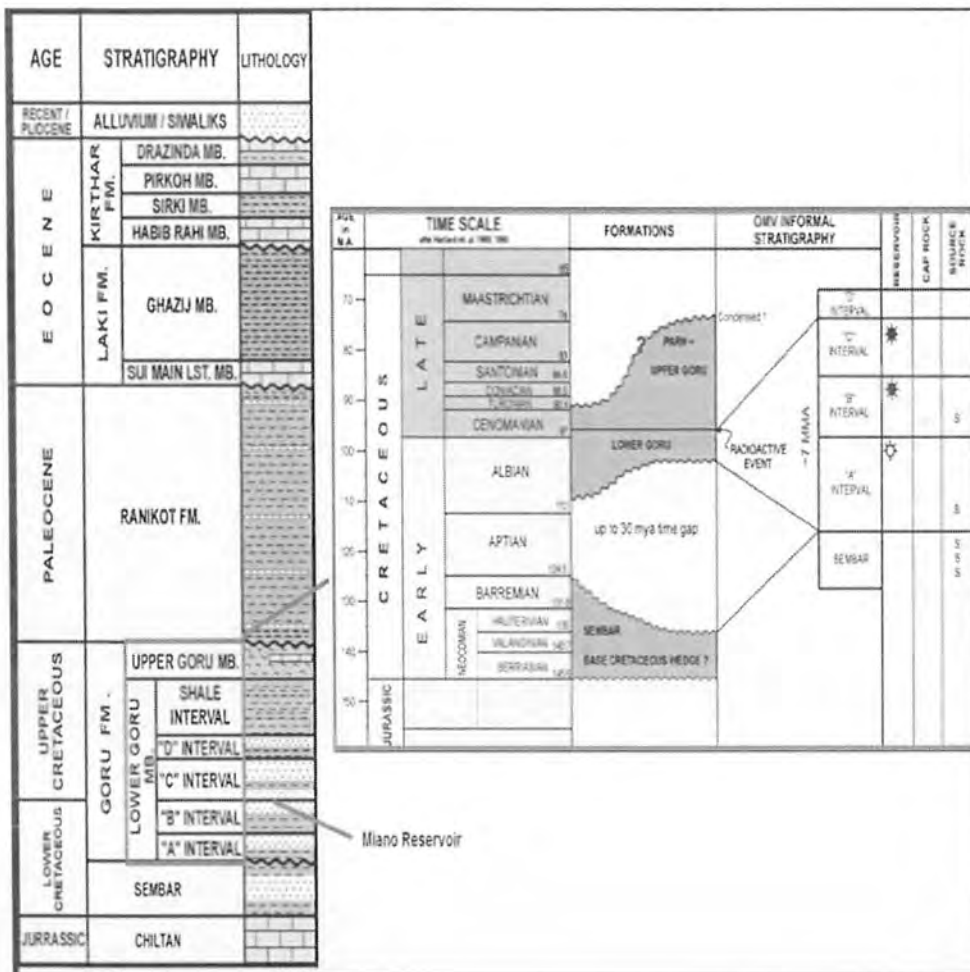


Figure 2.6 Stratigraphic column of study area (Mehmood et al., 2004)

### 2.6.1 Source Rock

Source rock is the productive rock for hydrocarbon. The Formations which act as a good source rocks in the study area are as follows:

- **Sember Formation**

Sember Formation is believed to be the major source of hydrocarbons in Central and Southern Indus basins. Potential of a reservoir also occurs within the sandstone part of the formation.

- **C-Interval of Lower Goru Formation**

As interbedded shale and sandstone layers are present in Lower Goru formation and shale act as a good source rock so in this assigned area lower Goru formation is divided into different interval and C Interval is one of the good source rocks of the study area.

All of the possible source rocks of the study area Sember is the best source for the largest production of oil and gas fields in Indus basin (Iqbal and Shah, 1980).

### **2.6.2 Reservoir Rock**

B-interval of lower Goru is considered as good reservoir rock of this area. Usually the depositional environment of the Lower Goru "B" sands in the Miano field is tide dominated and formation's lithology is the sandstone with the occasional beds of shale. Sandstone is white, yellowish brown in color. Its porosity ranged between 10-15% and patchy yellowish to bluish white fluorescence.

### **2.6.3 Seal Rock**

Seals act as a barrier for the flow of hydrocarbons. In the Central Indus Basin Upper Goru shale and interbedded shales of Sui Main Limestone of Cretaceous are acting as a seal but in study area C-interval of Lower Goru formation is acting as a good seal rock (Kadri, 1995). Thin beds of variable thickness act as an effective seals in producing fields.

### **2.6.4 Traps**

All production in the study area is from structural traps. The tilted fault traps in the study area are a product of extension related to rifting and the formation of horst and graben structures.

## CHAPTER 3

### SEISMIC INTERPRETATION

#### 3.1 Seismic Methods

Seismic Methods is the most authentic methods used now a day to locate hydrocarbon deposits, geothermal reservoirs, archaeological sites and groundwater to obtain geological information. It can provide information about the structure and distribution of rock types in the subsurface (Kearey et al., 2009).

##### 3.1.2 Seismic Reflection Method

In seismic reflection surveys seismic energy pulses are recorded which are reflected back from the subsurface interfaces. The travel times are measured and can be converted into estimates of depths to the interfaces (Kearey et al., 2009). Depth of reflecting interfaces can be estimating from the recorded time and velocity information that can be obtain either from reflected signal themselves or from surveys in well (Dobrin & Savit, 1988).

#### 3.2 Seismic Interpretation

Seismic interpretation implies picking and tracking laterally consistent seismic reflectors for the purpose of mapping geologic structures, stratigraphy and reservoir architecture. The ultimate goal of interpretation is to delineate hydrocarbon accumulation and their extent. Conventional seismic interpretation is an art which is required in geology and to geophysics to map the structures. Seismic interpretation can also be defined as “Transformation of seismic data into structural picture”. In simple words it is the process of determining the subsurface information of the earth from seismic data. It may determine general information about an area, locate prospects for drilling exploratory wells, or guide development of an already-discovered field (Coffeen, 1986).

### 3.3 Workflow for Seismic Interpretation

Procedure adapted for interpretation is given in Figure 3.1. Base map is prepared by loading navigation and Seg-Y data. The software used for this purpose is IHS kingdom. After preparing base map faults are identified on the basis of the geology of the area and interested horizons are also marked on the seismic section then by synthetic seismogram marked horizon are confirmed. Faults polygons are generated to see the structure present in the study area and horizons are contoured. The different important steps involved in the interpretation are discussed in workflow in the Figure 3.1.

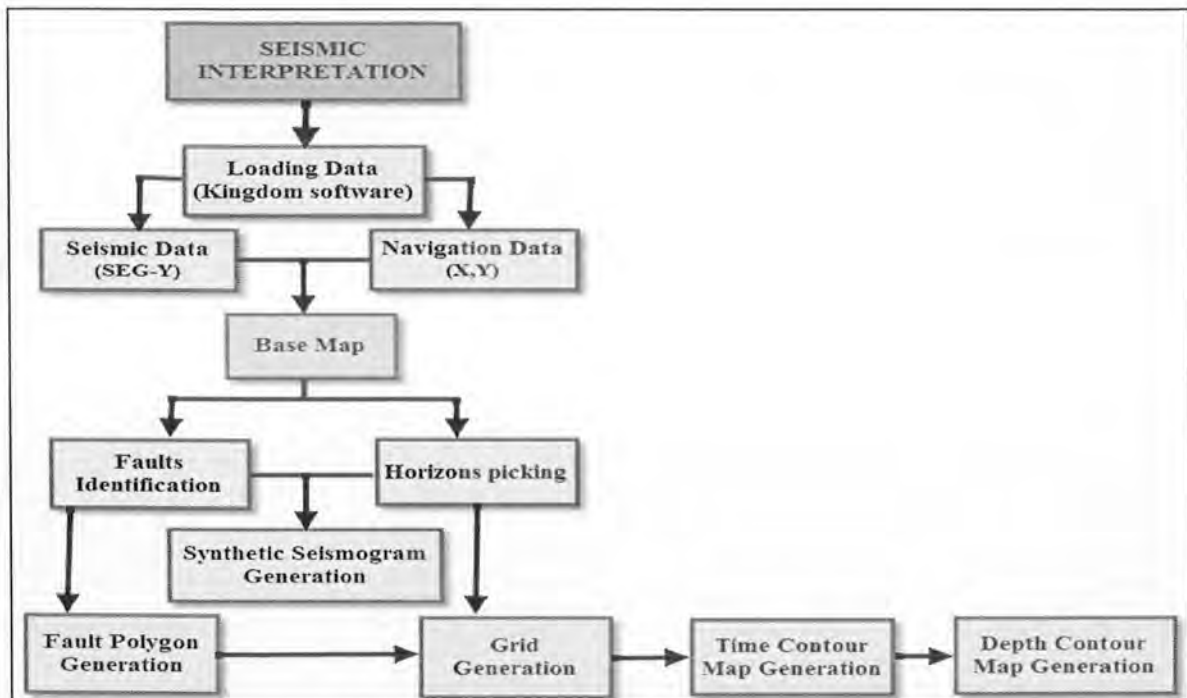


Figure 3.1 Work Flow of seismic interpretation.

### 3.4 Fault Marking

Conventional seismic interpretations are the arts that require skills and thorough experience in Geology and Geophysics to be precise (Mc. Quill in et al., 1984). Fault marking on real time domain seismic section is quite a hard work to do without knowing tectonic history of area (Sroor, 2010). Miano area is present in extensional regime horst and Graben structure formed. Knowing geologic history as discussed in chapter 2 in detail, the area under study must have normal faults trending North-South along each dip line (East-West).

### 3.5 Horizon Picking

Interpreting seismic sections, marking horizons, producing time and depth maps is a task which depends on interpreter's ability to pick and follow reflecting horizons (reflectors) across the area of study (Mc.Quillin et al., 1984). Reflectors usually correspond to horizon marking the boundary between rocks of markedly different lithology but it does not always occur exactly at geological boundary of horizon which is sometimes important problem in seismic interpretations (Kemal et al., 1991).

### 3.6 Interpreted Seismic Sections

Four lines were assigned to me for the completion of this dissertation i.e., P2094-214, P2094-216, P2094-219 and P2094-223. Five major Faults were marked named as F1, F2, F3, F4 and F5 and three Horizon were marked on the basis of reflector continuity and values from TD chart. Interpreted seismic sections are shown below in Figure 3.2, Figure 3.4, Figure 3.6, and Figure 3.7. In this study horizons on the seismic line P2094-223 were marked first then tie it with other lines to mark the horizons. At the tie point of both intersecting seismic lines have same horizons at the same time. If the horizons do not have same time then there may be mistie that may be removed later on. Taking seismic line P2094-223 as a reference line, all other seismic sections used in the study are marked. At the tie point we not only mark the horizons but faults are also marked in the same manner all the faults were correlated. Three horizons are marked and their time is given above:

Table 3.1 Time of the marked horizon

HORIZON	TIME(s)	DISPLAY COLOR
Lower Goru	1.61	Green
C Interval	2.08	Pink
B Interval	2.17	Gold

Figure 3.2 shows the interpreted seismic line (P2094-223 Horst and Graben structure is very clear from the Figures 3.2 and 3.5. Whereas time section of both dip lines are also incorporated which clearly shows the fault movement and displacement across faults. All interpreted Seismic sections are shown below in Figures 3.2, 3.3, 3.4, 3.5, 3.6, 3.7.

- Dip line P2094-223

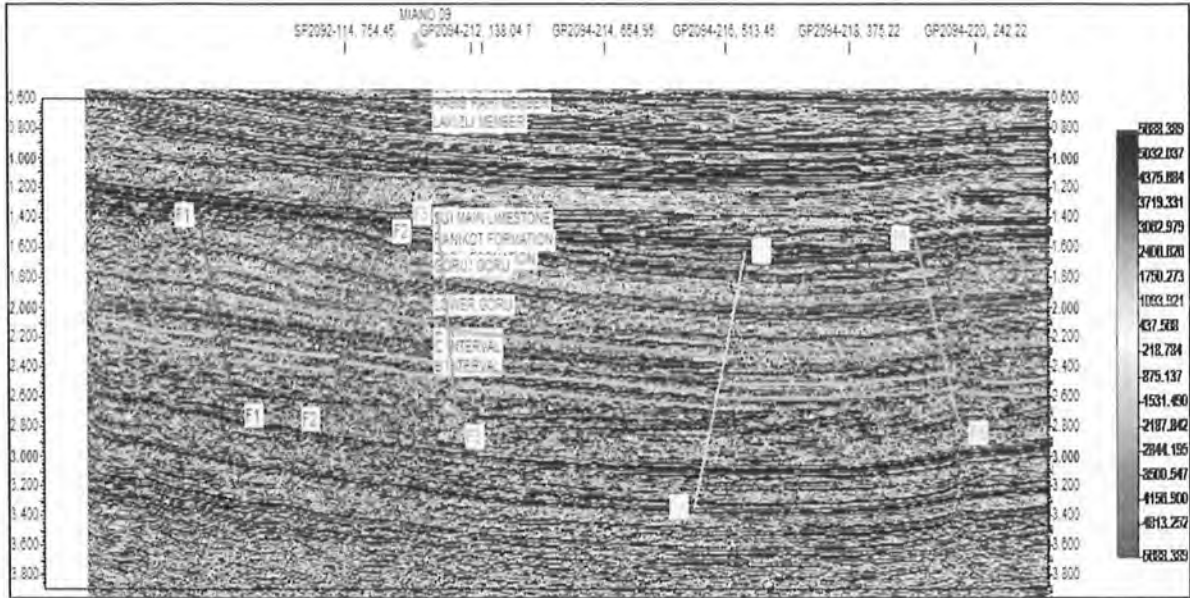


Figure 3.2 Interpreted time section of P2094-223.

- Time Section of Line P2094-223

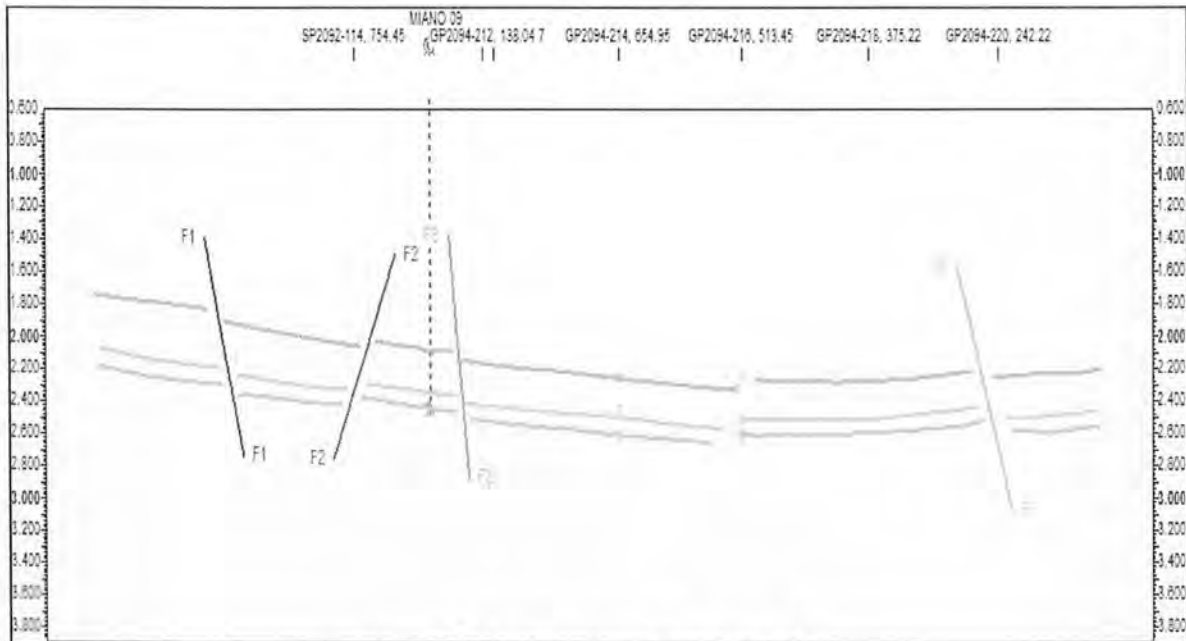


Figure 3.3 Depth section of line P2094-223.

- **Interpreted Dip Line P2094-219**

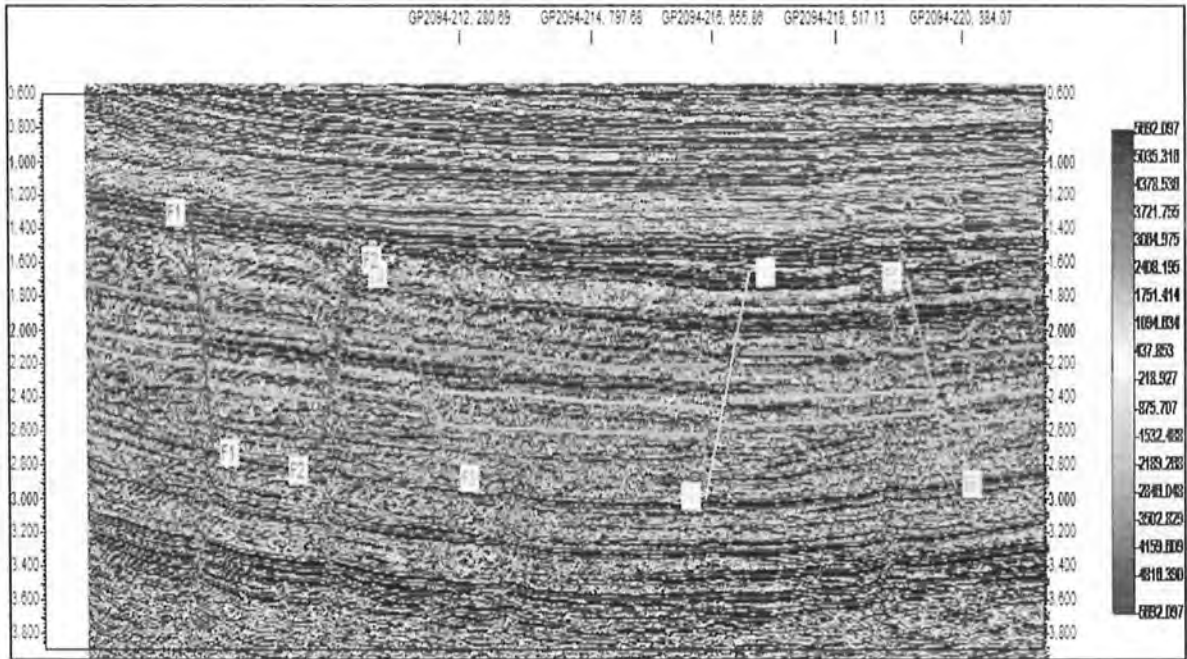


Figure 3.4 Interpreted time section of line P2094-219.

- **Time Section of Line P2094-219**

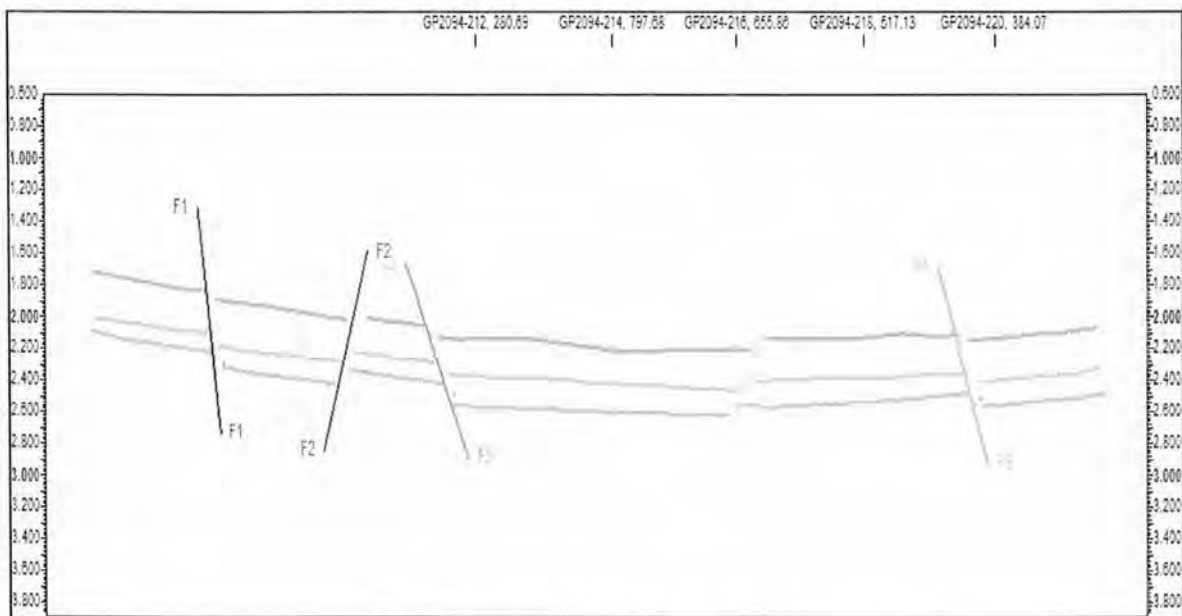


Figure 3.5 Depth section of line P204-219.

Now strike lines are interpreted below and shown in Figure 3.6 and Figure 3.7.

- **Interpreted lines P2094-214 and P2094-216**

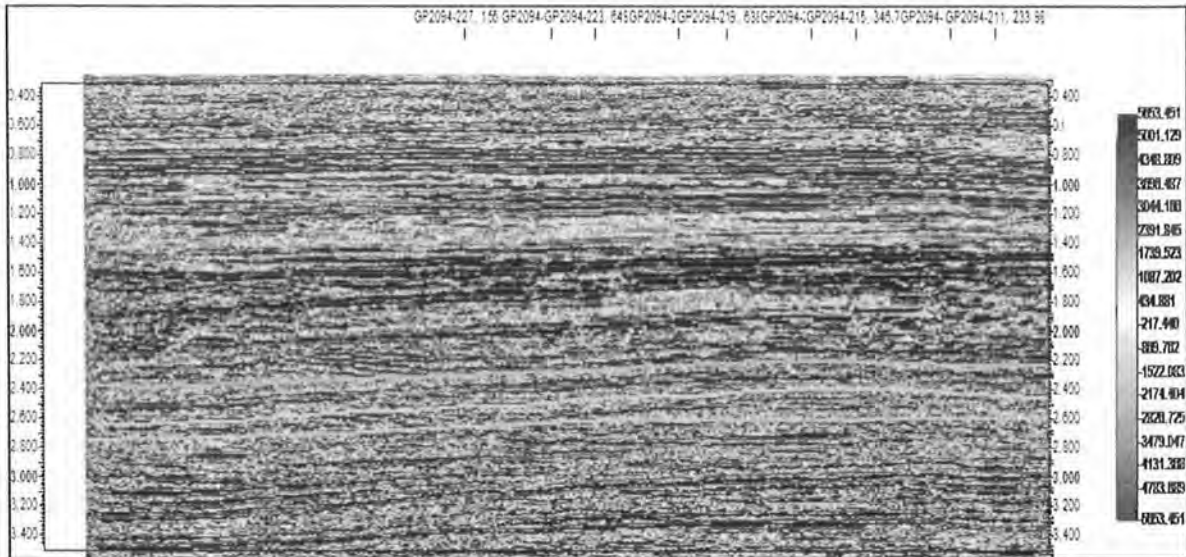


Figure 3.6 Interpreted strike line (P2094-214).

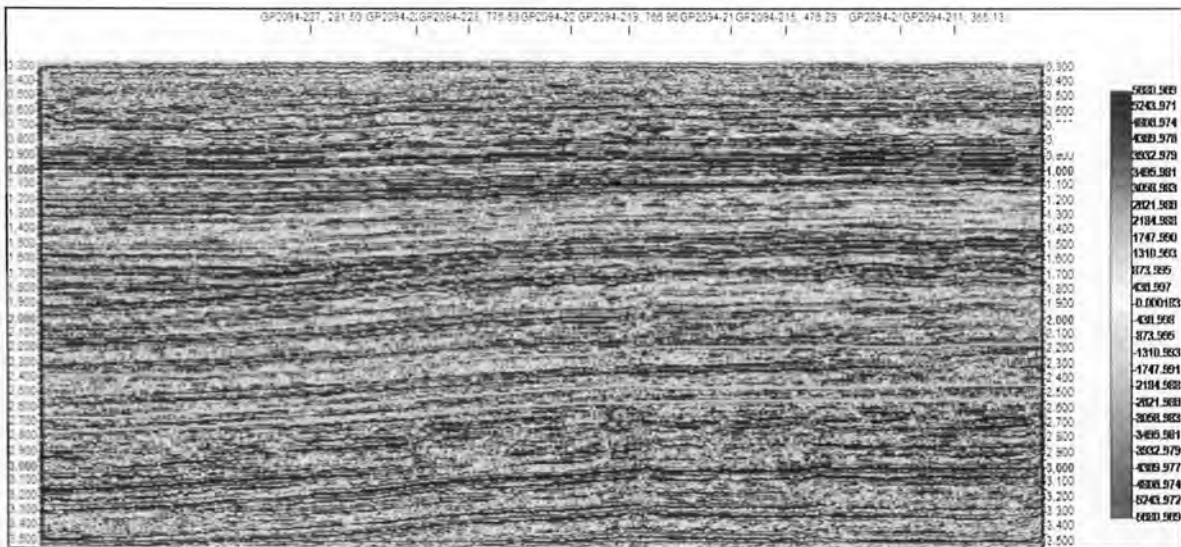


Figure 3.7 Interpreted strike line (P2094-216).

It is very difficult to identify faults on strike line and three horizons are marked on strike lines shown above in Figure 3.6 and Figure 3.7. After this interpretation Synthetic seismogram is generated to confirm the marked horizon. Synthetic seismogram of Miano-9 well is generated which lies on line P2094-223 and it confirms the marked horizons.



### 3.7 Generation of Synthetic Seismogram

Synthetic Seismogram is a result of one of many forms of forward modeling to predict the Seismic response of the Earth (Sroor, 2010). For 1-D forward modeling or synthetic seismogram generation, TWT (two way time) for each well top/reflector is required. From the well data, the depths of the formations are known, by plotting values of depths & times which came from the check-shot survey, we can extract the time value for certain depth ( to mark that depth on seismic section). However check-shot surveys are expensive and are not available for research purposes. Another way to find TWT is using Sonic Log Data. Impedance log can be generated by multiplying digital data of Sonic and density logs point by point, equation (01). From LAS files of wells available, Reflection Coefficient (RC) Series is calculated using this acoustic impedance (AI) log by using formula given in equation (2), after this a source wavelet(Ricker Wavelet or may be extracted) is generated and then this source wavelet is convolved with reflection coefficient series to generate a synthetic seismic trace, equation (3). Following are some basic information should be pointed out, carried during preparation of synthetic trace:

- Kelly Bushing was reference datum of survey
- The Check-shot time is two way time determined from well log data
- The type of well depth was MD (Measured Depth from KB)

Convolution of wavelets with RC series means the combination of both, source wavelet and reflection coefficient series shown in figure 3.8 and mathematically can be written as following:

- **Acoustic Impedance (I)=  $V_p(\text{Sonic log}) * \text{Density}(\text{Rhob}) = \rho v$**  (1)

- **Reflection Coefficient =  $(\rho_{2V2} - \rho_{1V1}) / (\rho_{2V2} + \rho_{1V1})$**  (2)

- **Seismic Reflection = Seismic source wavelet \* Earth reflectivity** (3)

- **Synthetic Seismogram = Artificial source wavelet \* RC-Series** (4)

Synthetic seismogram of Miano-9 is generated and it confirms the B-Interval of Lower Goru. Other lithologies are not identified due to data limitations. Synthetic seismogram of Miano-9 is shown below in Figure 3.9 which lies on line P2094-223.

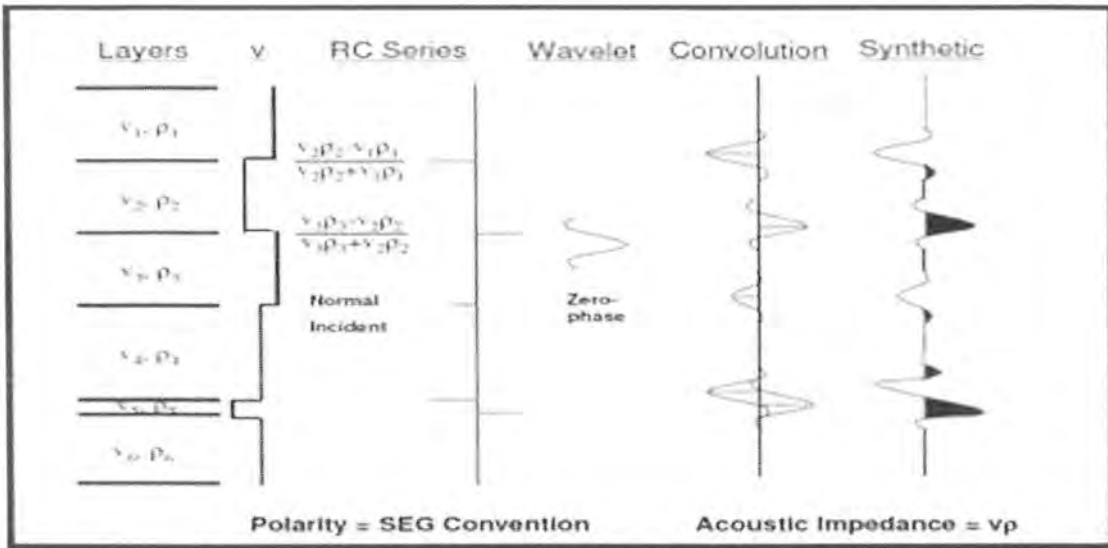


Figure 3.8 Process of convolution and making of synthetic seismogram (Courtesy IHS).

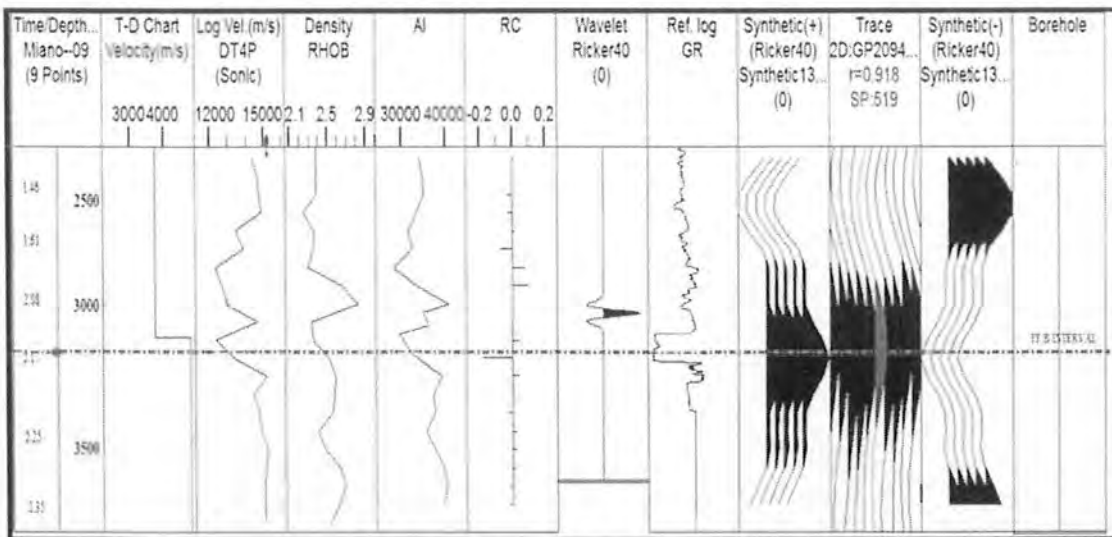


Figure 3.9 Synthetic Seismogram of Miano-9.

Synthetic seismogram is generated to know the exact location of the formation tops Picking in time domain, then, to tie it with the seismic section. Synthetic also indicates that whether the horizon response is peak or trough which is key clue for interpretation of relative acoustic impedance response of reflector (Sroor, 2010). In figure below Synthetic seismogram is shown which confirms the top of B-interval.

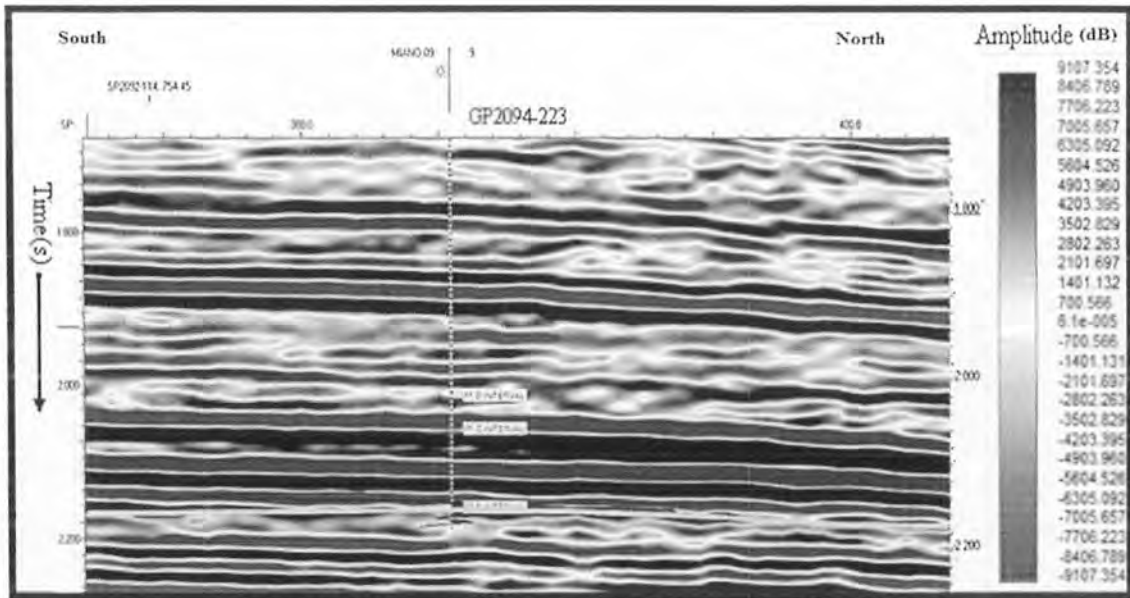


Figure 3.10 Correlating Synthetic with Seismic line P2094-223

All assigned lines are interpreted and next step is to generate Fault polygon and contours as synthetic seismogram confirms only B interval of Lower Goru formation so polygon and Contours of only B interval is generated.

### 3.8 Generation of Fault Polygon

We pick the fault on seismic section & find it at the other seismic lines. The fault in seismic section is called Fault Segment and the fault on map view is called Fault Polygon (Sroor, 2010). It is also generated to see the lateral extent of the faults on all seismic lines. In any software for mapping an area all faults should be converted in to polygons prior to contouring. The reason is that if a fault is not converted into a polygon then it is difficult for the software to recognize it as a barrier or discontinuities. In Figure 3.11 fault polygon of B-interval is shown.

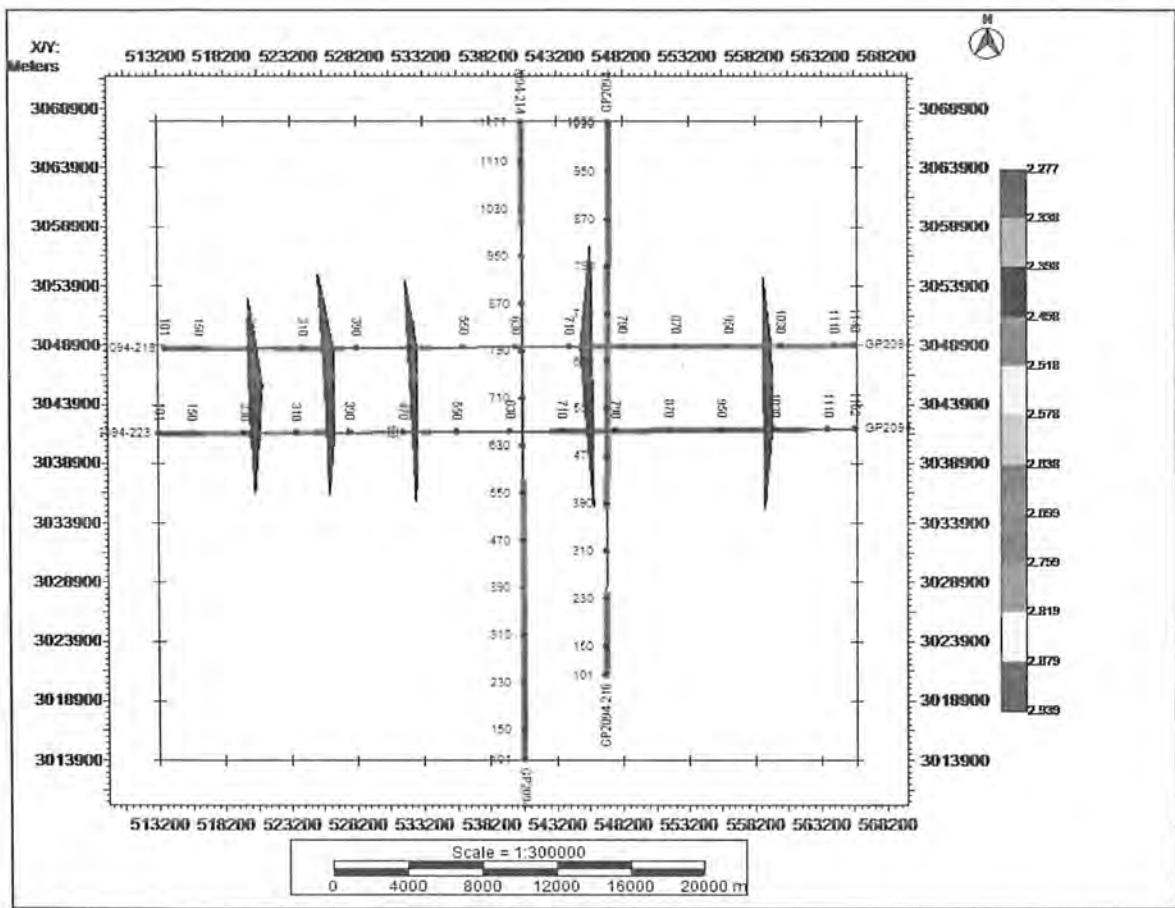


Figure 3.11 Fault polygon of B-interval.

### 3.9 Contour Map

In seismic interpretation contouring is used to identify the structure forming a particular horizon. For the purpose of constructing subsurface contour maps from the seismic data formation and reference datum is selected first. For the purpose of constructing subsurface contour maps from the seismic data formation and reference datum is selected first. The reference datum may be above or below sea level (Gadallah & Fisher, 2009).

#### 3.9.1 Time Contour Map

Time contour maps show lateral as well as vertical variations with respect to time at the level of horizons. Time contour maps are constructed on B-interval Figure 3.12 respectively. The pattern of Time Contour map confirms the shape of the subsurface structure. Time contour

maps of these formations show 2D-variations with respect to time and the hydrocarbons probably accumulate at those places where contour values are low.

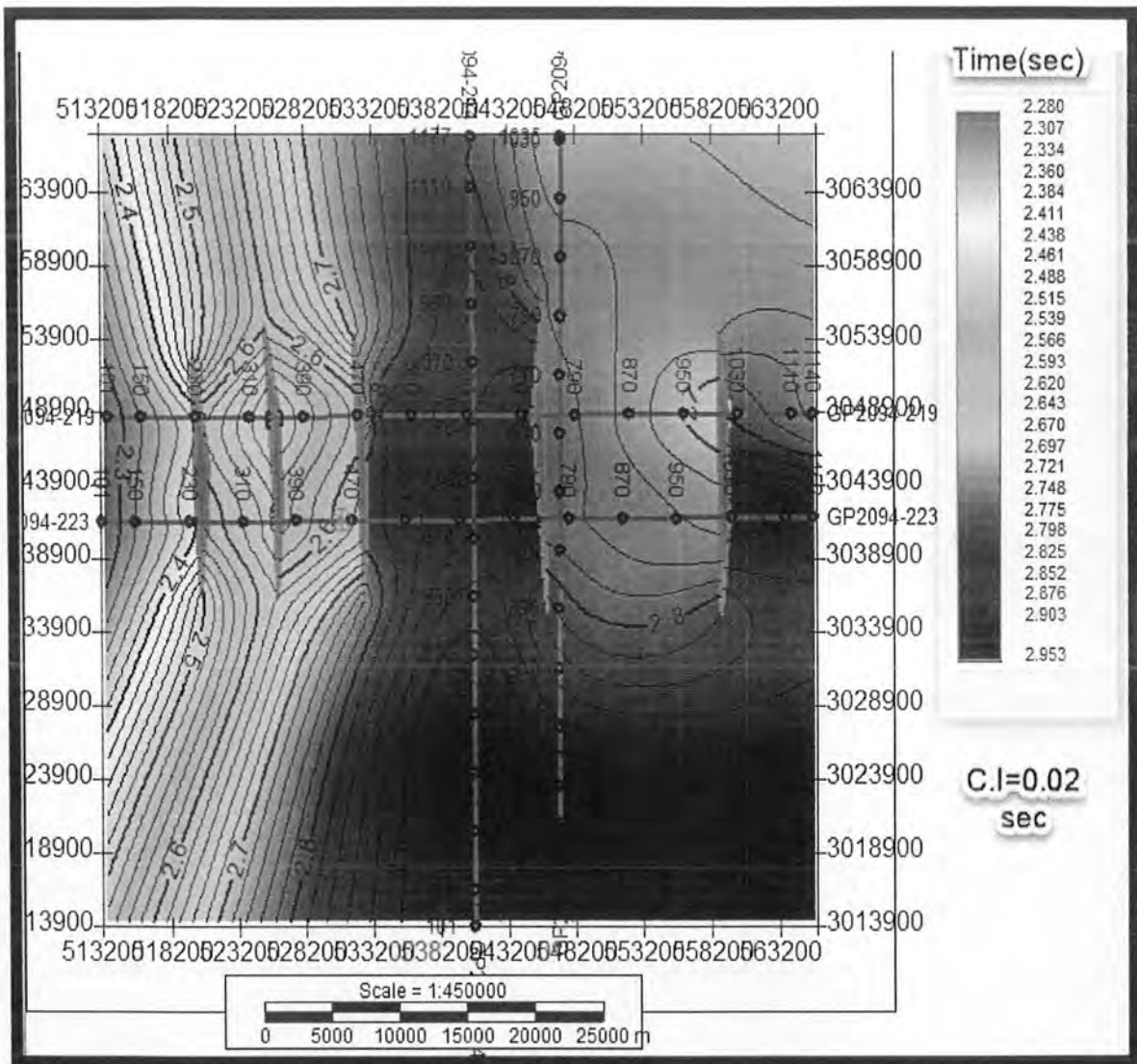


Figure 3.12 Time contour Map of B-interval.

It is clearly shown that Horst and Graben structure formed in the study area and the favorable place for hydrocarbon is horst and due to color variation and color bar it is clear that low values of time shows horst while high values of time are Graben.

### 3.9.2 Depth Contour Map

Depth contour maps also show lateral variation with respect to depth. For depth contour map velocity is required. After velocity analysis and evaluating a single velocity for the depth contour map all seismic sections as well as time contour maps have been converted into depth sections and contour maps by using true velocity from wells available in study area by using following formula;

$$S = (V) * T / 2, \tag{6}$$

where,

S = depth of Reflector in meters

V (well point) = velocity at well point in m/s

T = Two way travel time in seconds.

The depth contour map is generated by multiplying time contours and velocity contours. The trend of depth contour maps is same as of time contour maps because there are same lateral variations with time as well as depth. Depth contour maps of B-interval are shown in Figure 3.14 respectively. The pattern of both contour maps confirms the sub-surface shape of the structure present. The hydrocarbon may accumulate where the contour values are low because hydrocarbon accumulates at those places where there is low pressure.

Contouring pattern shows N-E region as relatively uplifted area. Structural pattern of the area also confirm by contouring as the horst and Graben geometry. From the Figures 3.14, it is clear that horsts and Graben structures are formed which is also formed in time contour maps. Lighter color shows relatively shallower part while darker color shows relatively deeper portion. In depth contouring map region shown in green color horst with low values of time might be the good zone for the accumulation of hydrocarbons because hydrocarbons move towards low pressure area.

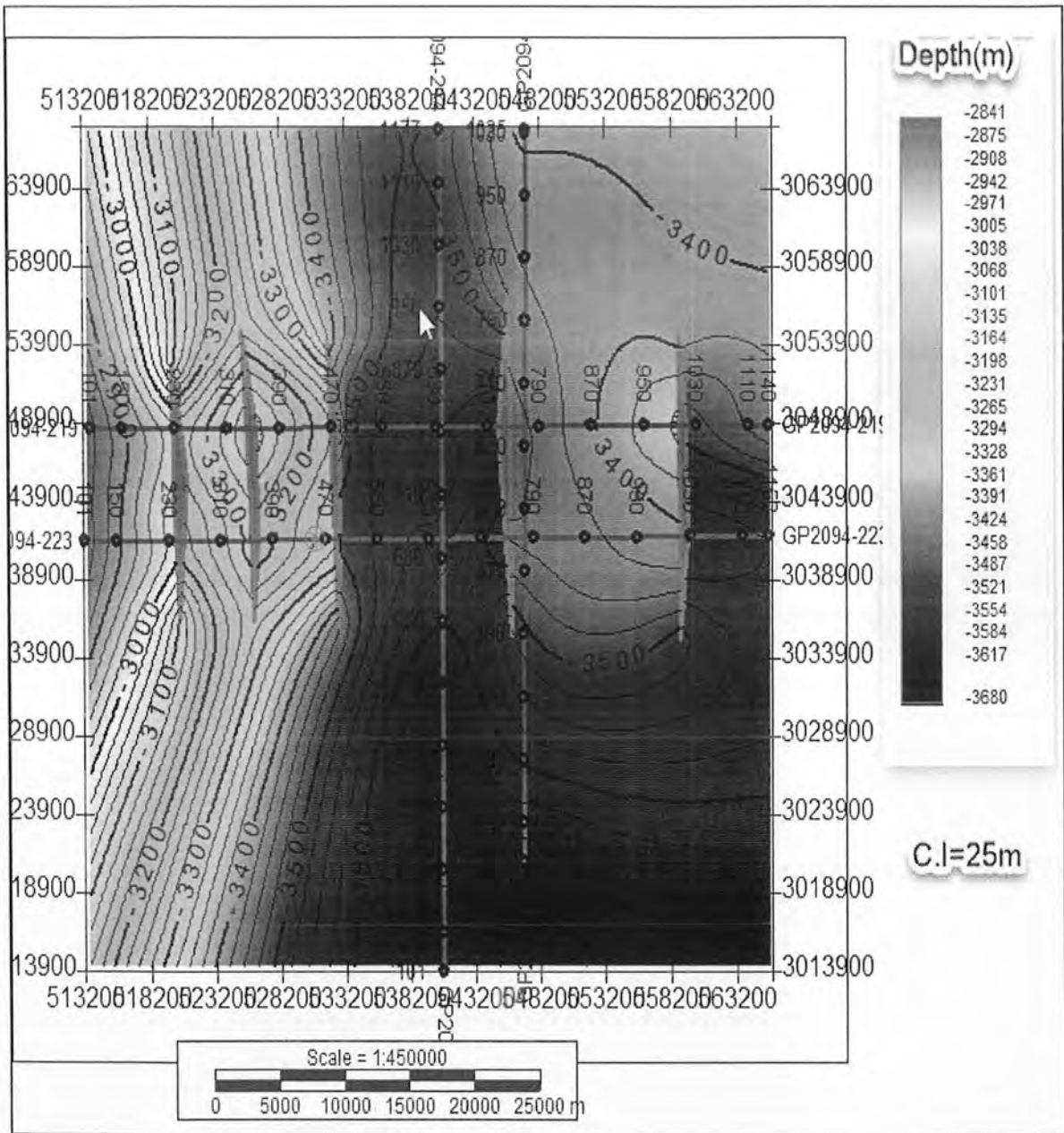


Figure 3.13 Depth contour map of B-interval.

## CHAPTER 4

### SEISMIC ATTRIBUTES

#### 4.1 Introduction

Seismic attribute analysis it provide some qualitative information of the geometry and confirms the seismic interpretation. From the early days of seismic prospecting, Explorationists usually used this single seismic data attribute to draw conclusion about subsurface geology. Attribute computations decompose seismic data into constituent attributes. Thus attributes are of many types: pre-stack, post-stack, inversion, velocity, horizon, multi component 4-D.

#### 4.2 Physical Attributes

Physical attributes relate to physical qualities and quantities. As the magnitude of the trace envelope is directly linked to acoustic impedance contrast; frequencies are related to wave scattering and specially to bed thickness whereas Instantaneous and average velocities directly related to rock properties (Taner, 1994).

#### 4.3 Geometrical Attributes

Geometrical attributes deals with the spatial and temporal relationship of all other attributes. Bedding similarity, lateral continuity and discontinuity is measured by semblance whereas bedding dips give depositional information of the area. It is also used for stratigraphical interpretation and also used to quantify features like depositional patterns, and related lithology (Subrahmanyam, 2008).

#### 4.4 Envelope of Trace on Line P2094-223

The Trace Envelope is a physical attribute and it can be used as an effective discriminator for the following characteristics (Subrahmanyam, 2008).

- Indicate possible gas accumulation with the help of bright spots
- Mainly represents the acoustic impedance contrast, hence reflectivity
- Thin-bed tuning effects
- Changes in depositional environment



- Unconformities
- Major changes of lithology

Trace envelope shown in figure 4.1. Line used for this purpose is P2094-223.



Figure 4.1 Envelope Attribute on line P2094-223.

## 4.5 Instantaneous Frequency

Instantaneous frequency attribute relates to the centroid of the power spectrum of the seismic wavelet (Subrahmanyam, 2008). Its uses include:

- Low frequency anomaly indicates Hydrocarbon presences.
- Abnormal attenuation and thin bed tuning is also identified (Chopra et al., 2005)
- Low frequency zones indicate fracture zones.
- Bed thickness indicator.
- Higher frequencies indicate sharp interfaces such as laminated shale, lower frequencies are indicative sand-prone lithology.
- Instantaneous frequency can indicate bed thickness and also lithology parameters.

- Identify weathered layer.

Information obtained from seismic data where frequency shows negative signs. It is due to the closely-arriving reflected wavelets (Figure 4.2). Here in Figure 4.2 instantaneous frequency is not completely confirming the interpretation done due to some data limitations.

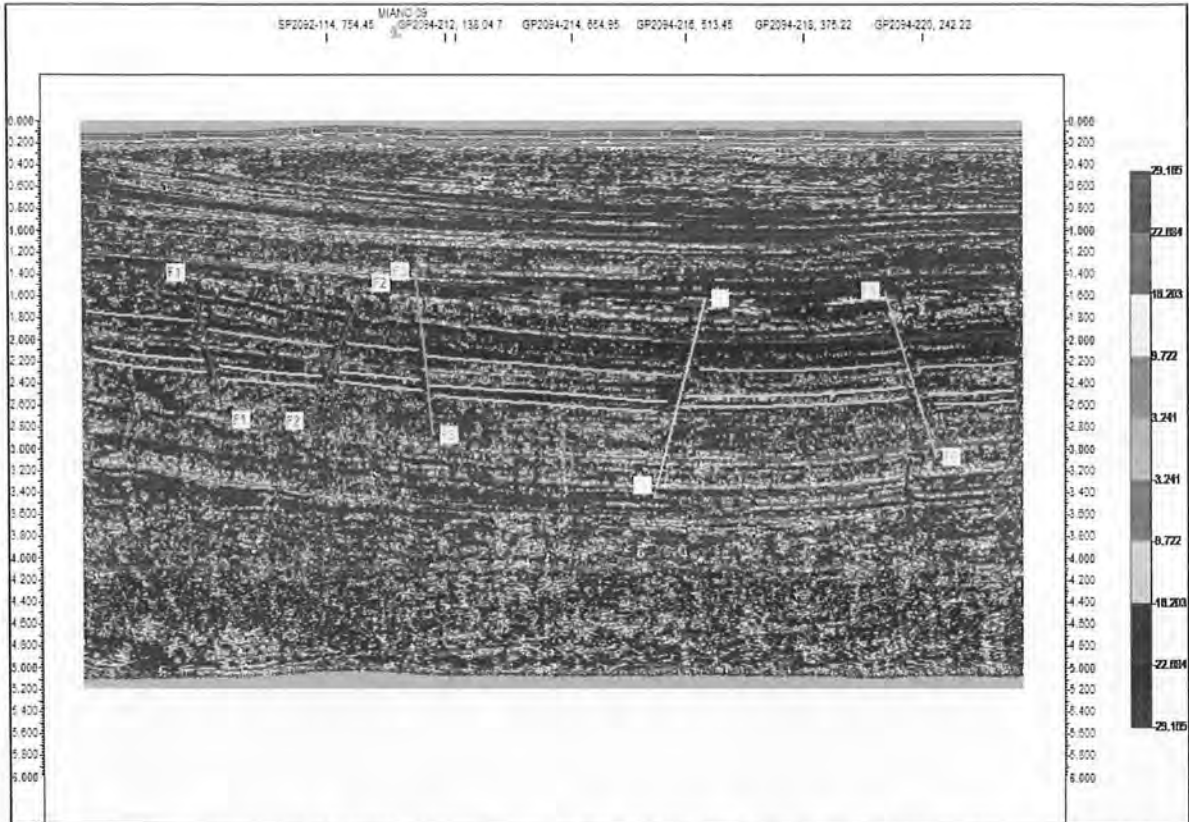


Figure 4.2 Instantaneous Frequency calculated for seismic line P2094-223.

#### 4.6 Instantaneous Phase

For tracking reflector continuity, faults identification and unconformities instantaneous phase attribute is used. Hence it confirms the reflectors and faults marked. The phase information obtained from phase attribute is independent of trace amplitude and related to seismic wave fronts (Figure 4.3).

The interpreted horizons lie over the zero phase regions indicated by white color. This attribute further confirms the interpretation as the input data is zero phase. The phase attribute in

Figure 4.3 show the lateral discontinuity and continuity and slightly confirms the interpretation done in chapter 3.

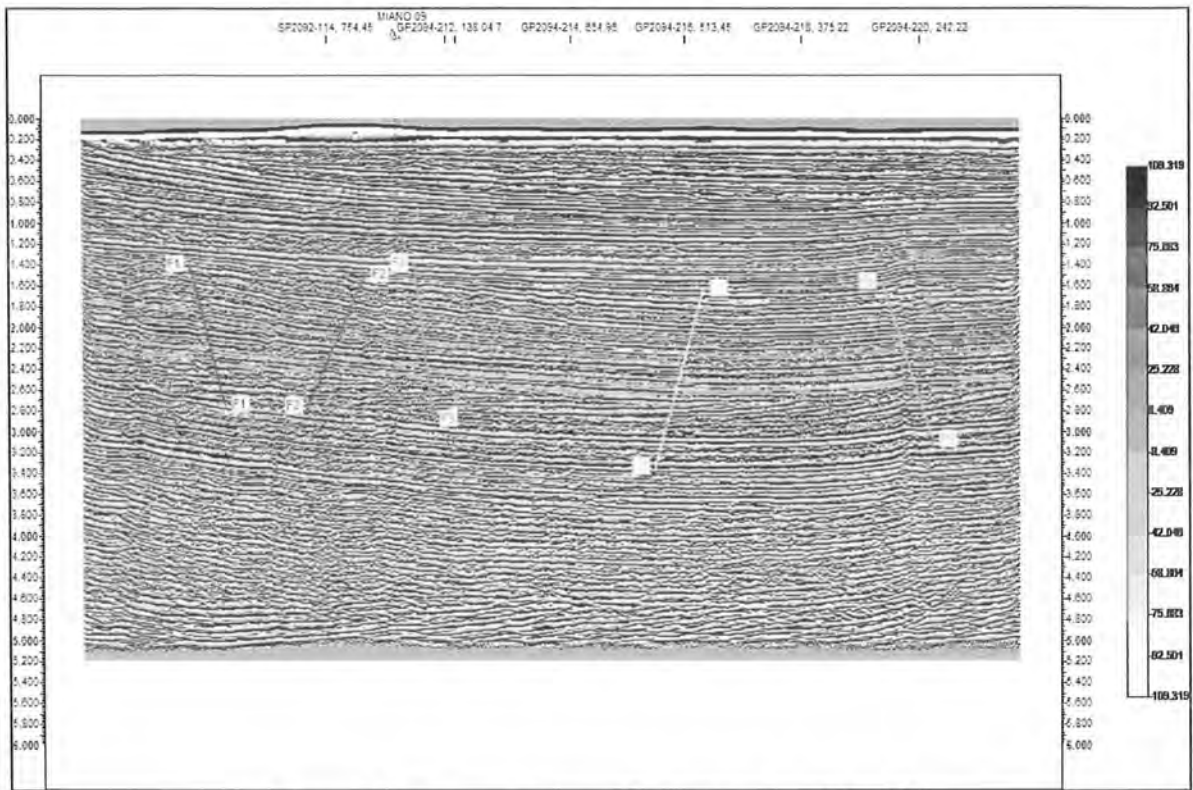


Figure 4.3 Instantaneous Phase calculated for line P2094-223.

## CHAPTER 5

### PETROPHYSICAL ANALYSIS

#### 5.1 Introduction

This chapter deals with the calculation of rock properties and techniques that relate the geological properties (e.g. porosity, lithology, saturation) of a rock with the corresponding elastic and seismic properties at certain physical conditions (e.g. pressure, temperature) termed as Rock Physics.

#### 5.2 Petrophysics

Petrophysics is the study of rock properties and their interaction with fluid contents (Djebbar Tia, 2004). When physical measurements of the rocks like core analysis is combined with log analysis then the work done is called petrophysical analysis. The geologic material used in the formation of reservoir for the accumulation of hydrocarbons in subsurface contain three-dimensional network of interconnected pores which the fluid content and allow the movement of the fluid within the particular formation (reservoir). Most important and useful tool available for the geophysicist and geologist is the Petrophysical log interpretation. Petrophysics give us idea about the following factors i.e.

- Productive zones of hydrocarbon are identified.
- Helps in defining Petrophysical parameters like porosity, permeability, hydrocarbon saturation and lithology of zones.
- Depth, thickness, formation temperature and pressure of a reservoir can be determined.
- Distinguish between oil, gas and water zones in a reservoir.
- Hydrocarbon mobility is also measured.

#### 5.3 Raw Log Curve

The Petrophysical analysis for reservoir characterization of Miano area has been carried out. For this purpose well data of MIANO-9 and MIANO-10 is used for the prospect, reservoir

generation and data was issued by DGPC (Directorate General of Petroleum Concessions). For Petrophysical analysis Caliper log, Gamma Ray log (GR), Spontaneous potential log (SP), Resistivity log and porosity logs are used.

Using these logs different rock properties can be measured which is the main objective of this chapter. These logs are identified or displayed in the Figure 5.1.

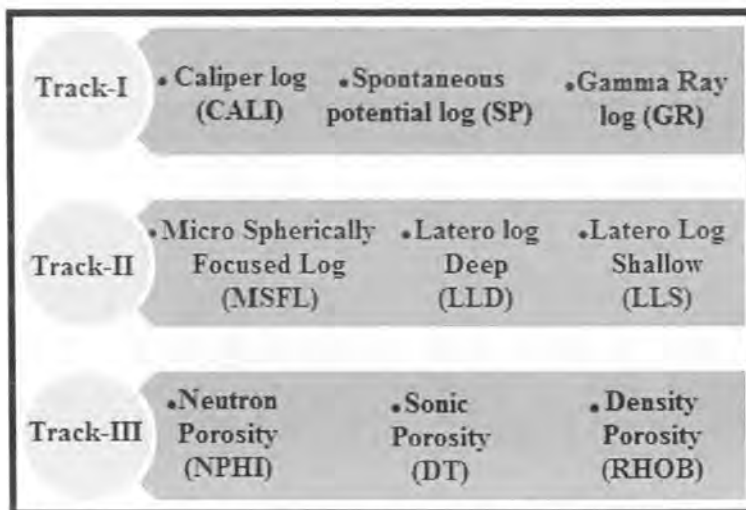


Figure 5.1 Basic three log Tracks.

### 5.3.1 Lithology Track

Gamma ray log, SP log and Caliper log is included in this track against the depth and every log has a linear scale. It reads the radioactivity of rocks in API units. Caliper log is a technical tool of logging which measures size and shape of borehole diameter. The SP is useful tool for the detection of permeable beds, marking bed boundaries and shale indicator (Schlumberger, 1974).

### 5.3.2 Resistivity Track

It includes MSFL, Latero log deep (LLD) and Latero log shallow (LLS). All of these logs are plotted on logarithmic scale due to more variations in resistivity (1-1000ohm) with depth. Formation resistivity and water saturation of rock is measured through this log.

### 5.3.3 Porosity Track

This track is also called track 3 and it includes the Sonic (DT), Density (RHOB) and Neutron log. These logs give us the porosity of the formation or rock present in the well.

### 5.4 Work Flow for Petrophysical Interpretation

The log data of Miano-9 and Miano-10 is available in Logging ASCII Standard (LAS) format. The log curves parameters given in the LAS file header are used to calculate all basic and advance parameters. The methodology adopted for this work is given in Figure 5.2 and each analysis step is discussed in the proceeding sub-sections. For calculating rock properties IHS kingdom software is used in which first we load the well data then define tracks and the full procedure is carried out which is shown in Figure 5.2 in which first define tracks then calculate different parameters of rocks for both wells Miano-9 and Miano-10 and then mark the hydrocarbon zone and required result is obtained shown in Figure 5.6 and 5.7.

The following rock properties are calculated in this chapter:

- By means of gamma-ray log presence of reservoir rock is identified.
- Net sand and net pay calculation.
- Volume of shale.
- Porosity determination.
- Water Saturation.
- The detection of hydrocarbon bearing zone

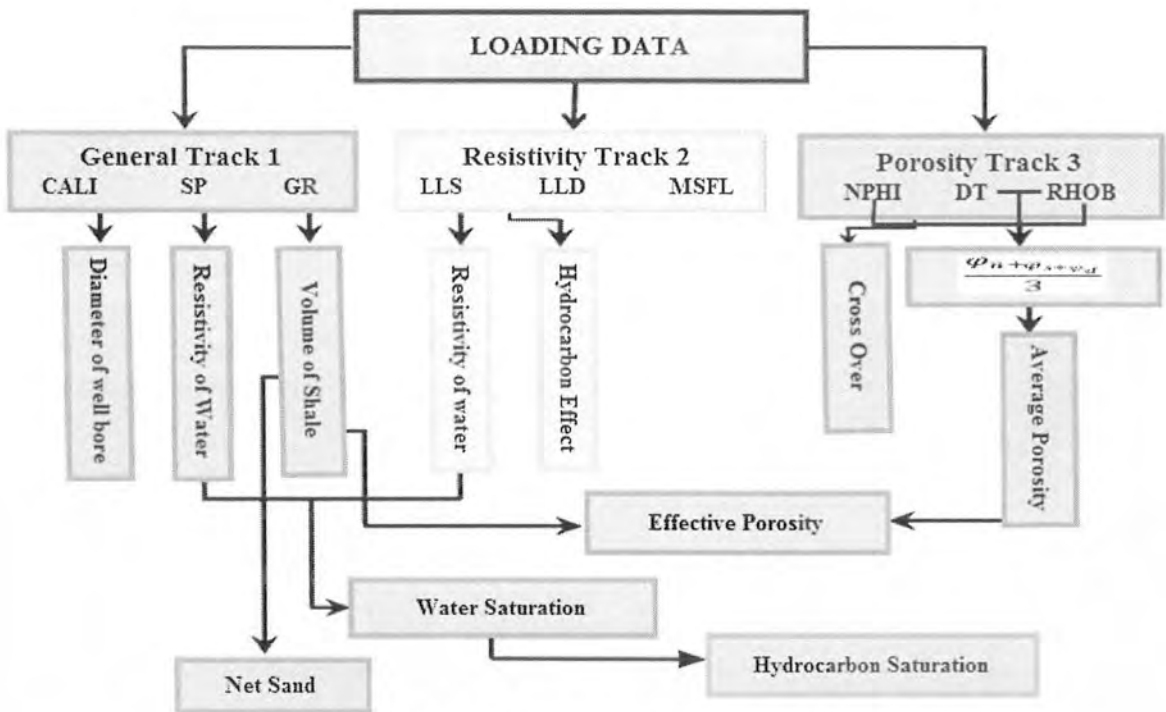


Figure 5.2 Work flow for petro physical analysis.

## 5.5 Calculating Rock Properties of wells Miano-9 and Miano-10

IHS kingdom software is used for calculation of rock properties of wells. As through Petrophysics we estimate the properties of reservoir so in Miano-9 properties of B-interval is calculated and its depth ranges from 3317feet to 3385feet.

### Depth Ranges of Miano-9 and Miano-10

Table 5.1 Shows depth ranges of wells

Sr.No	WELL NAME	TOTAL DEPTH OF WELL (m)	DEPTH OF B INTERVAL (m)
1	MIANO-9	3385	3331-3385
2	MIANO-10	3610	3317-3506

### 5.5.1 Volume of Shale

GR log basically used to find the VOLUME OF SHALE (VSH). Shale content reads high GR value whereas; sandstone or limestone shows lower value of GR (schlumberger, 1989).

$$VSH = \frac{(GR \log - GR \min)}{(GR \max - GR \min)}, \quad (1)$$

where,

VSH = Volume of shale

GR min = Minimum value of GR log in particular zone of interest

GR max = Maximum value of GR log in particular zone of interest

GR log = Value of GR log at given point in zone of interest.

Plot/log curve of volume of shale (VSH) of reservoir (B-interval) is shown in Figure 5.6 in track-5.

### 5.5.2 Porosity Calculation

- **Sonic Porosity**

The porosity of B-interval (interested zone) can be calculated using all porosity logs. Sonic log is useful technique which uses transit time to evaluate porosity of the formation. The interval transit time ( $\Delta T$ ) is dependent upon both lithology and porosity of the medium. Therefore, a formation's matrix velocity given must be known to calculate sonic porosity by the following formula given by (Wylie et al., 1958). Sonic porosity has been calculated by using this formula:

$$\Phi S = \frac{(\Delta T - \Delta T \text{ mat})}{(\Delta T f - \Delta T \text{ mat})} \quad (2)$$

where,

$\Phi S$  = Sonic porosity  $\mu s/ft$

$\Delta T$  = Log response

$\Delta T \text{ mat}$  = Transit time in matrix

$\Delta T f$  = Transit time in fluids.



According to Wyllie interval transit time ( $\Delta T$ ) increased due to the presence of hydrocarbon (i.e. hydrocarbon effect). In order to correct this Hilchie suggested the following empirical correction equation 3 and 4 for hydrocarbon effect. (Hilchi., 1978).

$$\Phi = \Phi_s \times 0.7 \text{ (for gas),} \quad (3)$$

$$\Phi = \Phi_s \times 0.9 \text{ (for oil),} \quad (4)$$

- **Neutron Log**

Neutron log gives the direct measurement of porosity. It is considered the concentration of hydrogen ions (HI) and pores filled within that formation (Asquith and Gibson, 2004). In clean formation (shale free formation), only the liquid filled (water or oil) are measured by this log (Schlumberger, 1974).

- **Total Porosity**

Total porosity can be calculated by the help of following formula. Sonic porosity and neutron porosity is used for calculating total porosity.

$$\Phi_T = \frac{\phi_s}{2\phi_n} \quad (5)$$

where,

$\Phi_T$ = Total Porosity

$\Phi_n$ = Neutron porosity

$\Phi_s$ = Sonic Porosity.

Plot of Total porosity is shown in Figure 5.6 and Figure 5.7 in track 7.

- **Effective porosity**

It is defined as “the ratio of the volume of interconnected pore in a rock unit to the total volume of the rock by removing the shale effect in that rock unit. The following relation is used for the determination of effective porosity (Asquith and Gibson, 2004).

$$\Phi_e = \frac{\Phi_s + \Phi_n}{2} * (1 - V_{sh}), \quad (6)$$

where, in equation 6:

$\Phi_e$  = Effective porosity

$V_{sh}$  = Shale volume.

Plot of effective porosity of Miano-9 and Miano-10 is shown in Figure 5.6 and Figure 5.7 in track 8.

### 5.5.3 Water Saturation ( $S_w$ )

It may be defined as “the percentage of the effective pore volume that is filled by the water in the formation”. It is calculated by using the following formula given in equation 7 known as Archie equation.

$$S_w = \sqrt[n]{\frac{F \times R_w}{R_t}},$$

(7)

where, F is the formation factor written as

$$F = \frac{a}{\phi^m}$$

(8)

$R_w$  = Resistivity of water

$R_t$  = True formation resistivity

$n$  = The saturation exponent its value is 2 taken but varies between 1.8 -2.5

$a$  = 1 for sandstone ,  $\phi$  = effective porosity

$m$  = Cementation factor and 2 for sandstone.

So it is evident from eq. 7 that to evaluate saturation of water we have to calculate  $R_w$ .

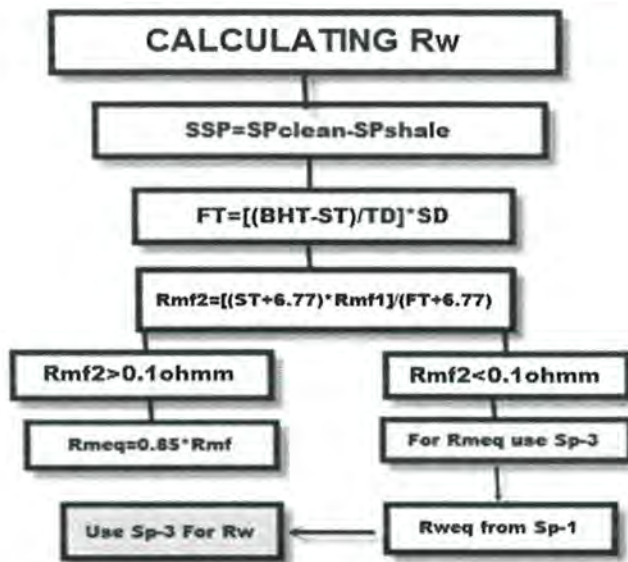


Figure 5.3 Workflow for calculating Rw.

Figure 5.3 shows all steps for calculating Rw to find water saturation.

1. Calculated Spontaneous Potential (SSP) which is -30mili volts for Miano-9 and Miano-10.
2. Find Formation temperature.

$$FT = \left[ \frac{(BHT-ST)}{TD} \times SD \right], \quad (9)$$

where,

BHT= Bore hole temperature

ST= Surface temperature

FD= Formation depth

TD = Total depth are taken from well header.

3. Then find Resistivity of mud filtrate (Rmf2) and formula is shown below in Figure 5.3 then we calculate Resistivity of mud filtrate equivalent (Rmef) using schlumberger chart 3(Sp-3).

Rmeq for miano-9 using Sp-3=0.025

A value of Rmeq and Rmf is shown in Figure 5.4.



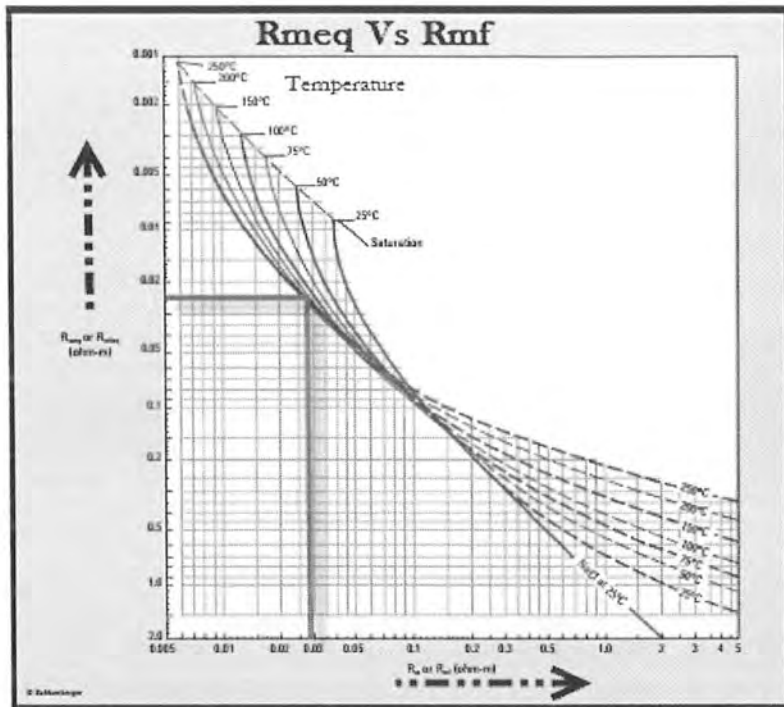


Figure 5.4 Schlumberger chart showing value of Rmeq.

4. Then calculate Rweq from Sp-1 where SSP= -30 so after finding this again use Sp-3 for Resistivity of water (Rw).

$$R_w = 0.017 \Omega\text{m}$$

So putting this value of Rw in eq. 7 we get Sw (saturation of water).

Sp-1 and Sp-3 charts are shown below showing calculated value of Rw.

This is the whole procedure through which we calculate saturation of water.

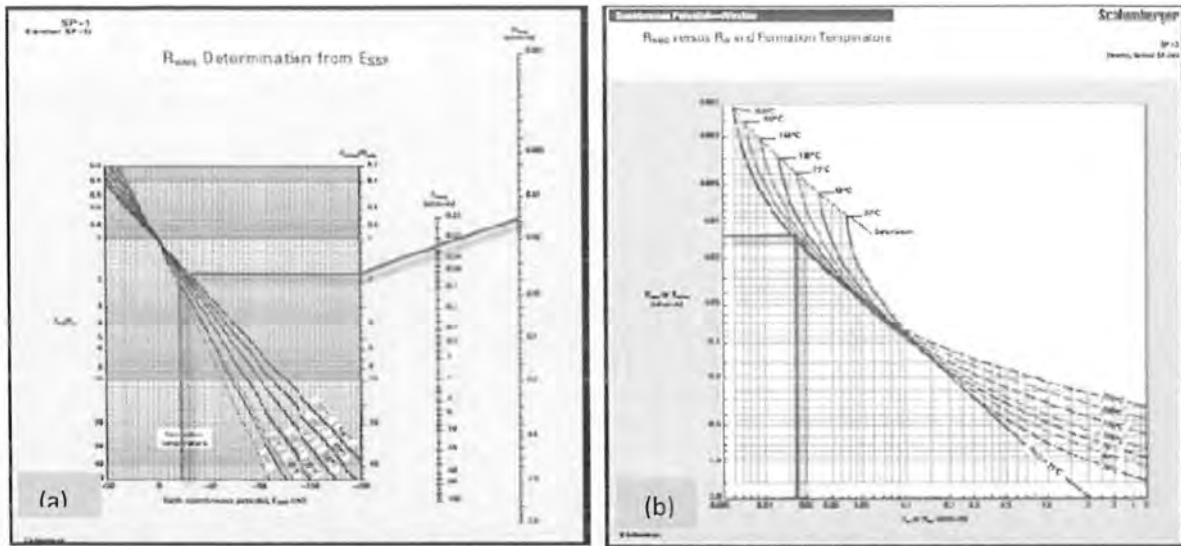


Figure 5.5(a) Calculated value of  $R_{eq}$  Sp Chart-1. (b) Calculated value of  $R_w$ .

### 5.5.4 Hydrocarbon saturation ( $S_h$ )

It is defined as the hydrocarbon present in the fraction of pore spaces. Hydrocarbon saturation can be calculated by using the equation 10.

$$S_h = 1 - S_w, \tag{10}$$

where,

$S_h$ =Hydrocarbon saturation

$S_w$ =Water saturation.

Plot of Hydrocarbon saturation of Miano-9 is shown in Figure 5.6.

### 5.6 Well Interpretation of Miano-9

IHS kingdom is used for interpretation of well Miano-9 and Miano-10. B interval of Lower Goru is reservoir of Miano-9 and its depth or thickness range is 3331-3385 feet. The well bore diameter will increased due to the collapsing of the well bore and the irregularity effect commonly known as Rugosity. So if at depth ranges Rugosity are present then log values are not consistent. As mentioned above that all rock properties are calculated and on the basis of those properties and on the behavior of logs we mark the possible hydrocarbon zone. Zone A is the possible hydrocarbon portion of B interval of as shown in figure below (Figure 5.6).

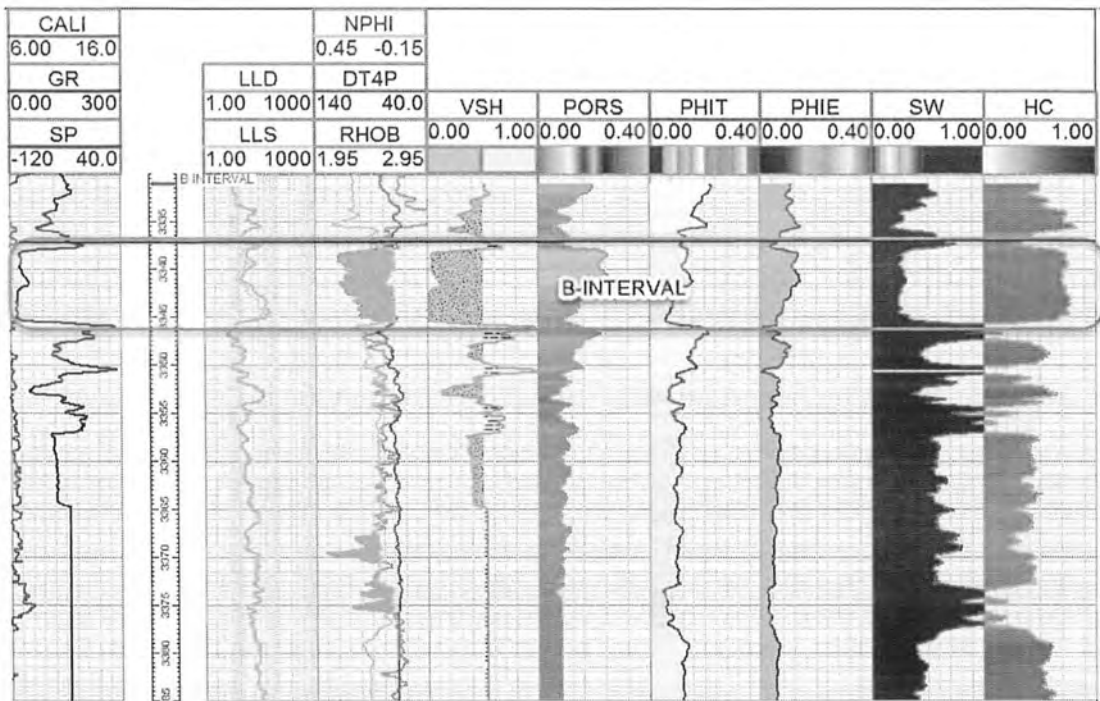


Figure 5.6 Petrophysical analysis of Miano-9.

Table 5.2 Calculated parameters of ZONE-A of B interval of MIANO-9

SR.No.	CALCULATED PARAMETERS	B-INTERVAL(m) (3331-3389)	Zone-A (m) (3337-3347)
1	Average Volume of shale= $Vsh_{avg}$	44%	24%
2	Average porosity from Sonic $\log=\phi_{Savg}$	11.3%	18%
3	Total porosity(PHIT)= $\phi_{avg}$	11.8%	12%
4	Average Effective porosity= $\phi_{eavg}$	6.4%	8%
5	Average Water saturation= $S_{wavg}$	51.7%	38%
6	Average Hydrocarbon saturation = $S_{havg}$	47.2%	62%

## 5.7 Well Interpretation of Miano-10

Same procedure is carried out for the interpretation of well Miano-10. Plot shown in Figure 5.7.

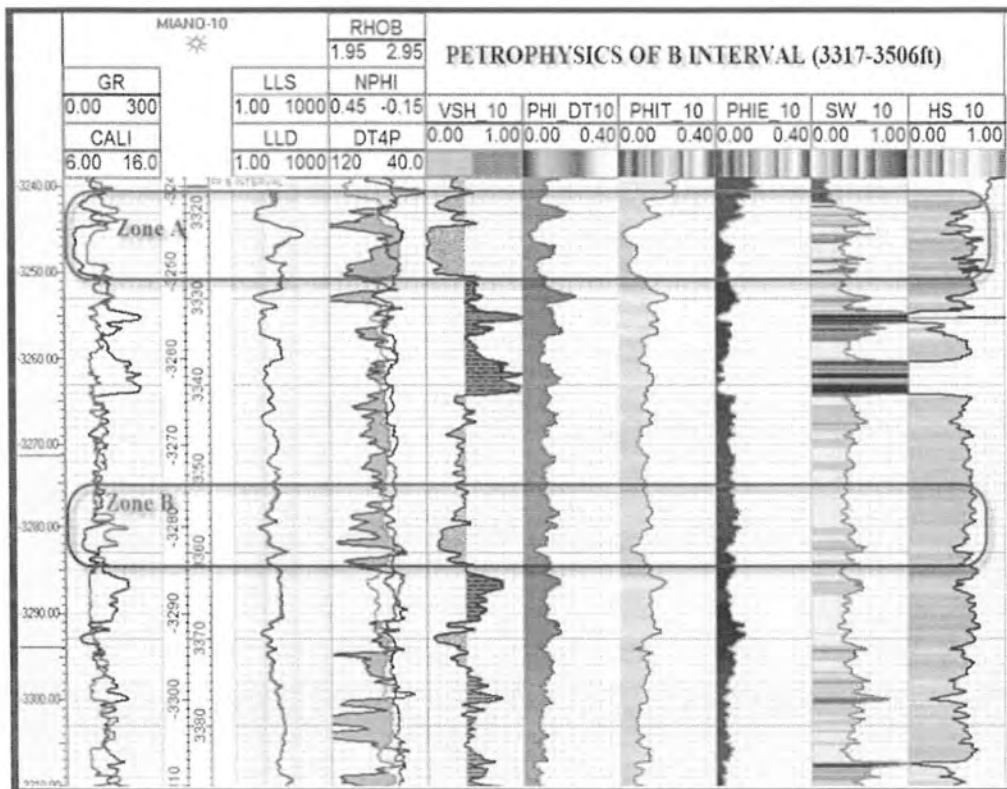


Figure 5.7 Petro physical analysis of Miano-10.

Table 5.3 Calculated parameters of B-interval of Miano-10

Sr. No.	CALCULATING PARAMETERS	B-INTERVAL(m) (3317-3506)	ZONE-A (m) (3318-3328)	Zone-B(m) (3352-3362)
1	Average Volume of shale= $V_{sh_{avg}}$	51%	28%	26%
2	Average porosity from Sonic log= $\phi_{S_{avg}}$	10%	10%	8%
3	Total porosity(PHIT)= $\phi_{avg}$	10.5%	7%	9%
4	Average Effective porosity= $\phi_{e_{avg}}$	10%	8%	9%
5	Average Water saturation = $S_{w_{avg}}$	40%	32%	34%
6	Average Hydrocarbon saturation = $S_{h_{avg}}$	60%	58%	62%

## Chapter 06

### Rock Physics

Rock physics is the term that contains the techniques that relate the geological properties of the rock with the corresponding elastic and seismic properties under certain physical conditions (Dewar, 2001).

- Rock Physics uses the porosity logs and also the shear velocity logs.
- The aim of the rock physics is to establish P-wave ( $V_p$ ), S-wave ( $V_s$ ) velocities, density and their relationship with elastic moduli.
- Rock Physics gives idea about velocities and elastic parameters.
- Rock Physics may use information provided by the Petrophysicist, such as shale volume, saturation levels etc. (Dewar, 2001).

#### 6.1 Estimation of Rock Physics

For the estimation of rock physics and engineering properties velocity function is used. But in earth there is variation in velocity vertically as well as laterally. So instead of using regional velocities interval velocities are used. By analyzing interval velocities we can compute different engineering properties (white, 1983). In this dissertation rock properties are estimated by using well log data. Primary velocity ( $V_p$ ) is computed by using sonic log. The following are the engineering properties. Properties are calculated for well Miano-9. Work flow to calculate Rock properties is shown below in Figure 6.1.

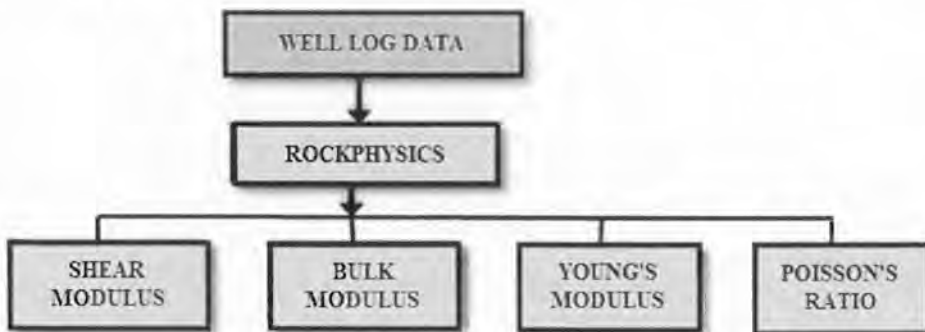


Figure 6.1. Work flow for calculating rock properties.



## 6.2 Seismic Waves and Elastic Moduli

Seismic waves traveling through the earth create small, short term, strains in the rock that lie in the elastic regime of the rocks. Therefore, using the relation of stress and strain we're able to calculate useful elastic moduli such as Young's modulus and Poisson's ratio (Rickman et al., 2008) or the LMR (Lame's modulus, shear modulus, and density) parameters (Good way et al., 1997).

### 6.2.1 Shear Modulus

The ratio of shear stress to the shear strain (angle of deformation). It is concerned with the deformation of a solid when it experiences a force parallel to one of its surfaces while its opposite face experiences an opposing force (such as friction). It describes the material's response to shearing strains relation moduli.

$$\mu = \rho * V_s, \tag{11}$$

where,

$\mu$  = Shear modulus

$\rho$  = Density and  $V_s$

S-wave = velocity.

### 6.2.2 Bulk Modulus

The bulk modulus (K) of a substance measures the substance's resistance to uniform compression. It is the ratio of volume stress to volume strain. It is calculated by using relation as under.

$$K = \rho(V_p^2 - \frac{4}{3}V_s^2), \tag{12}$$

### 6.2.3 Young's Modulus

Young's modulus is the stress needed to compress the solid to shorten in a unit strain. It can be defined as "Ratio of uniaxial stress over uniaxial strain in the range of stress in which Hook's law is valid. It can be computed as;

$$E = \sigma / \epsilon, \quad (13)$$

where,

E = Young's modulus

$\sigma$  = Tensile stress

$\epsilon$  = Tensile strain.

#### 6.2.4 Poisson Ratio

Poisson's ratio, sometimes denoted by the Greek letter small sigma ( $\sigma$ ), is a somewhat neglected elastic constant. In particular, Poisson's ratio for an isotropic elastic material is simply related to the P-wave ( $V_p$ ) and S-wave ( $V_s$ ) velocities of the material by

$$\sigma = \frac{0.5(v_p^2 - 2v_s^2)}{v_p^2 - v_s^2}, \quad (14)$$

This equation indicates that Poisson's ratios may be determined dynamically using field or laboratory measurements of both  $V_p$  and  $V_s$ . Poisson's ratio, named after Siméon Poisson, also known as the coefficient of expansion on the transverse axial, is the negative ratio of transverse to axial strain (Ivanov et al., 2006).

Plots of these properties of well Miano-9 are given below in Figure 6.3 in which properties of B-interval is calculated.

### 6.3 Rock Properties of Miano-9

Plot of all calculated properties are shown in Figure 6.3. In petrophysical analysis on the basis of log curve interested zone are marked for Miano-9 is from 3337-3347m shown in above Figure 6.3 while estimating Rock physics of this zone we end up with the conclusion that low values of young's, shear, bulk modulus,  $V_p/V_s$  and Poisson's ratio confirms our marked zone as hydrocarbon bearing zone. Rock properties were calculated to confirm the marked zone and to check the behavior of these properties in this zone.

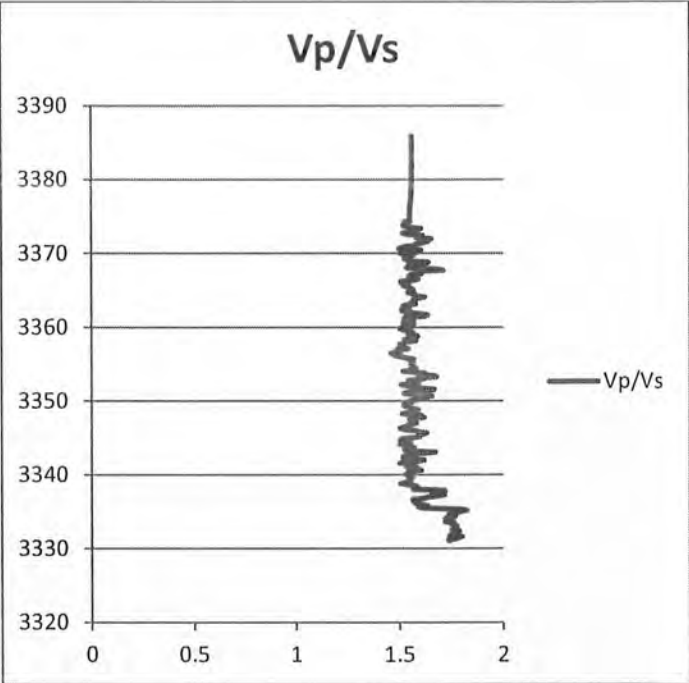
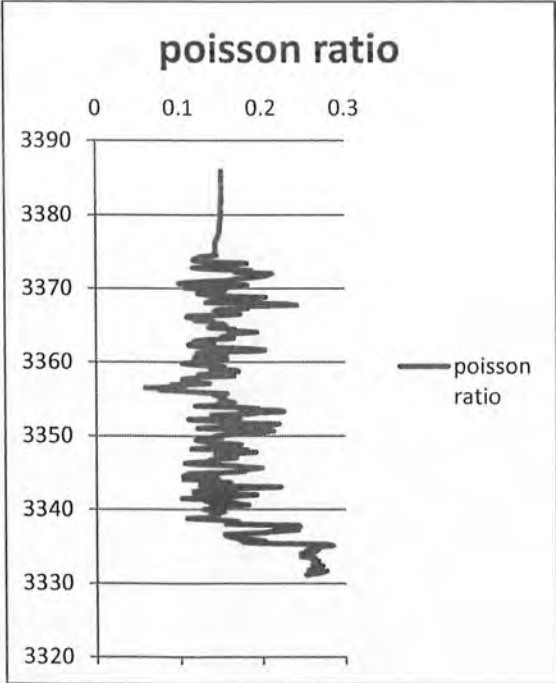
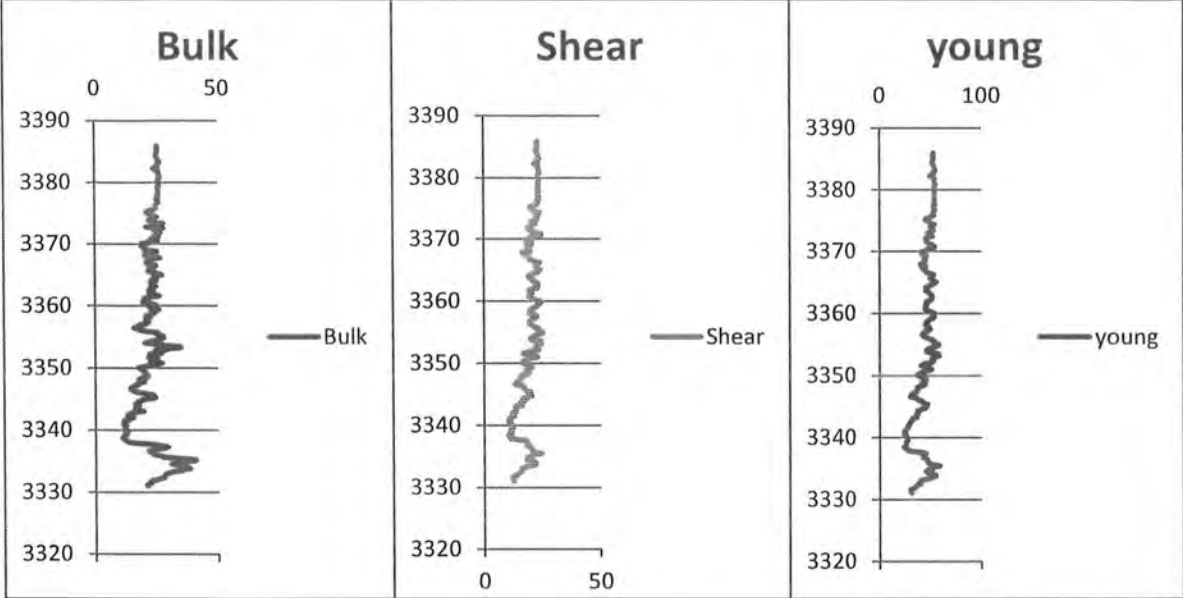


Figure 6.3 Behavior of rock properties calculated for well Miano-9.

## CHAPTER 7

### FACIES ANALYSIS

#### 7.1 Introduction

Facies are generally considered as bodies of rocks that show some specific characters but ideally these are rock units that form under certain conditions of sedimentation, displaying a particular process or environment of deposition (Staton, 1987). Facies models provide additional aid to the understanding of sedimentary environments and the origin of old sedimentary rocks (Johnson, 2004).

In linked with petro graphical and lithological variation different kinds of facies are identified on the basis of structure, composition and sedimentary texture (Ahmad et al., 2002). Different types of sedimentary environments are known like Transitional, terrestrial, continental slope, slope, and basin .Transitional (shoreline) environment include delta, beach, lagoon and tidal flat environments. Delta of transitional environment is deposited at mouth of river that caused coastline to swell into standing body of water. Marine environment include coral reefs and submarine facies (Rais et al, 2012) shown in Figure 7.1.

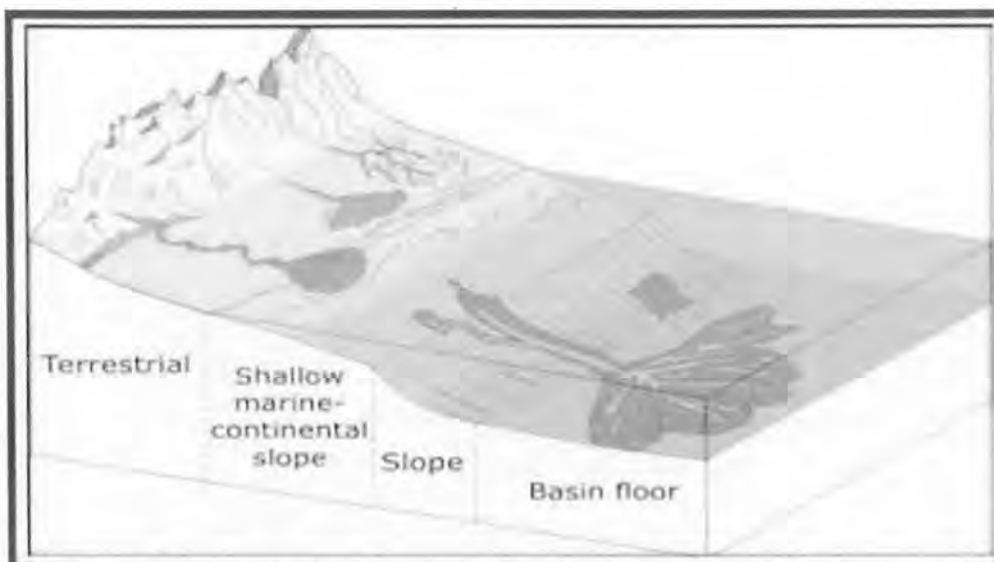


Figure 7.1 Major depositional environments ( Rais et al., 2012).

## 7.2 Walther's Law of Facies

In 1894, a German geologist in person of Johannes Walther proposed that Facies that occur in conformable vertical successions of strata also occur in laterally adjacent environments. Conversely, it states that when a depositional environment "migrates" laterally, sediments of one depositional environment come to lie on top of another. Walther's law applies to marine transgressions and regressions. However, the law is not applicable where the contact between different lithologies is non-conformable (Lucia, 1995). In Figure 7.2 procedure of Walther's law is clearly shown in which sediments of one depositional environment lie on top of another.

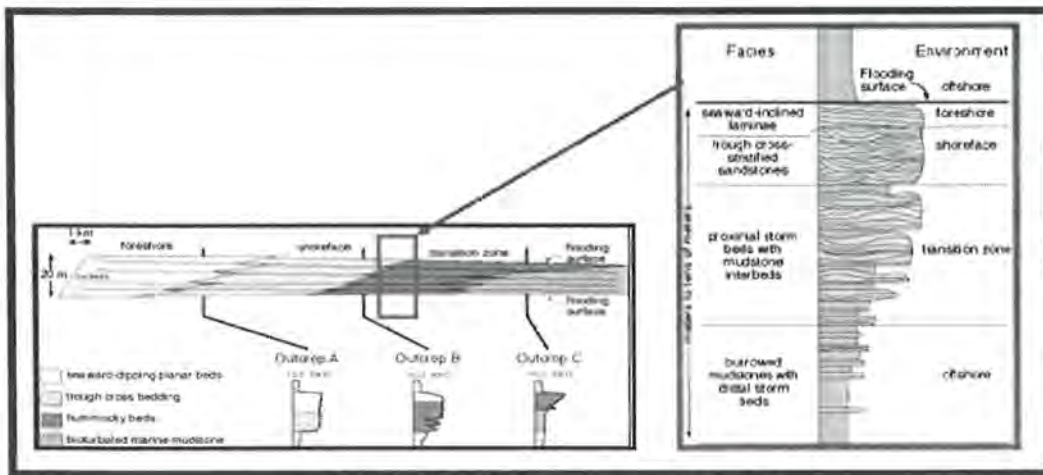


Figure 7.2 Depositional setting proposed by Walther.

## 7.3 Facies Analysis

Fundamental to all subsurface geologic studies is an analysis of depositional facies. Lucia (1995) describes development of a facies classification scheme is a particular challenging interplay between capturing enough information for environmental interpretation yet remaining simple. Particularly important is the characterization of facies such that their recognition criteria relate to critical environmental thresholds such as sea level, normal wave base, and storm wave base. These physical environmental zones regulate sedimentary textures and biotic assemblages. Depositional textures in turn affect porosity permeability in carbonates (Lucia, 1995).



### 7.3.1 Procedure of Facies Analysis

IHS kingdom software is used for Facies analysis and the workflow is shown below in Figure 7.3.

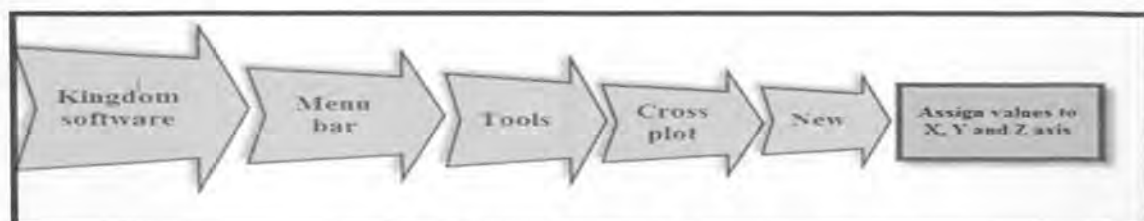


Figure 7.3 Workflow for Facies analysis.

By assigning different log data to the axis different cross plots will be obtained. Data of well Miano-9 is issued by DGPC and facies analysis of these two wells are shown below.

### 7.3.2 Facies Analysis of Well Miano-9

Facies analysis of B-interval of lower Goru has been done. Lower Goru formation is of cretaceous age and it is mostly composed of shale and interbedded sand stone. Initially facies analysis is done for whole Lower Goru formation from 2261m to 3385m and then performed for the zone ranging 3331 m to 3385m that also include B-sand or B-interval. Different cross plots are obtained by assigning different log data to the axis(X, Y and Z).

#### 7.3.2.1 Plot between Neutron porosity and Interval velocity of B interval

Three log curves are used for the facies modeling that are (Neutron porosity) NPHI (value ranges from -0.12 to 0.45) on x-axis, DTCO (value range from 51 to 90) on y-axis and (Gamma Ray) GR measured as count per second and its range is 15 to 290 in API is coded on z-axis and GR log is taken as reference log where depth range is from 3300 to 3400 for B sand. Cross plot obtained is shown below in Figure 7.4.

From the figure three facies has been identified and their lithologies are named as Sand, Shale and Shaly sand. GR log is taken as reference log and on the basis of the behavior of the three logs lithologies are identified as low values of DTCO, NPHI and low values of GR log behavior give indication of Sand. Through Facies modeling we are able to distinguish different lithologies present in reservoir.

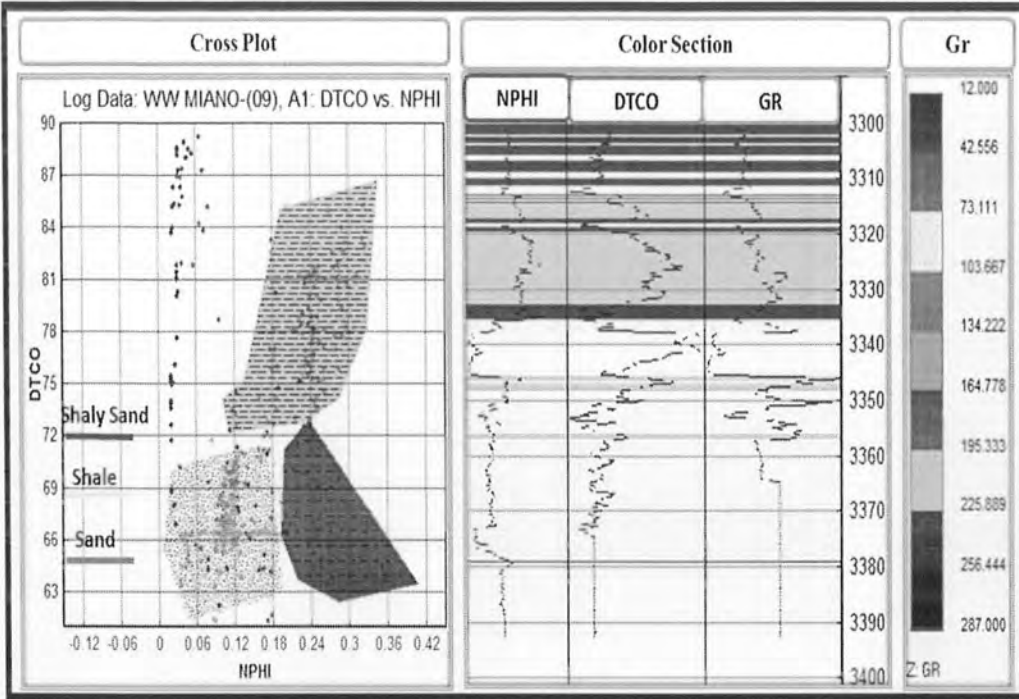


Figure 7.4 Facies analysis between DTCO and NPHI.

### 7.3.2.2 Plot between Neutron porosity and Density porosity of B interval

Now NPHI (neutron porosity), RHOB (density log) and Depth is taken as three log data where on x-axis NPHI (values -0.12 to 0.45) is taken, on y-axis RHOB (density log and value ranges from 1.95 to 2.95) is taken where depth is on z-axis and its values ranges from 3331 to 3385 which is depth interval of B-interval of Lower Goru formation in Miano-9. Plot is obtained which is shown in Figure 7.5.

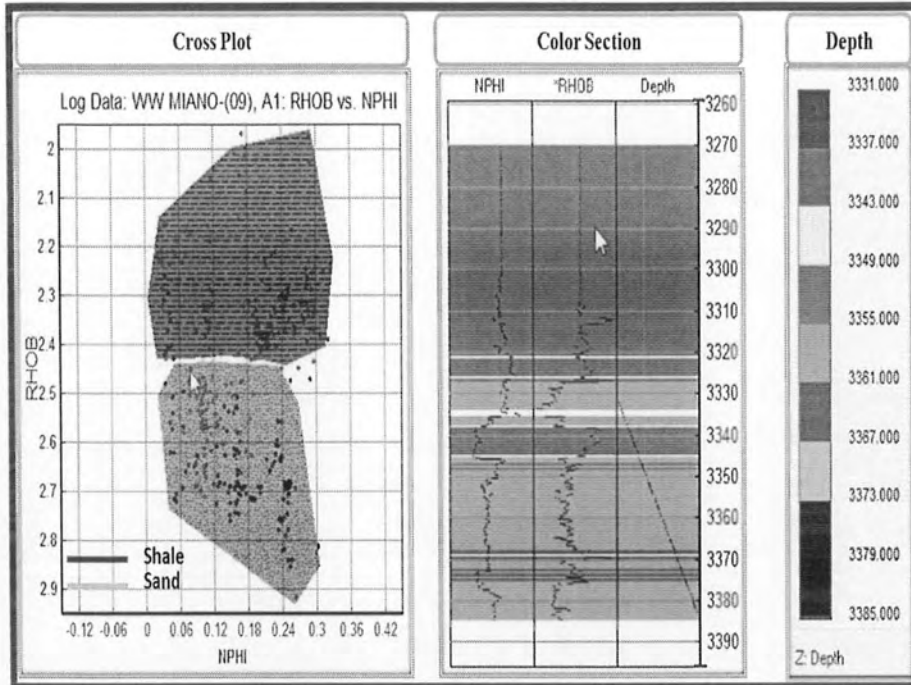


Figure 7.5 Facies analysis between NPHI and RHOB.



## Discussions and Conclusions

Basically major portion of this research work are: Structure interpretation of seismic data, seismic attribute analysis, Petro physical analysis, estimation of rock physics, facies analysis. From seismic data and well log data on the basis of general stratigraphic column present in the area three reflectors are marked which are shown in Figure 3.2, 3.4, 3.6, 3.7 respectively and marked horizons are B-interval, C-interval and Lower Goru and these horizons are confirmed with the help of synthetic seismogram of well Miano-9 on line P2094-223.

Five faults are marked which are normal faults depend on geology and tectonics of area. Normal faulting shows that area is in extensional regime and horst and Graben structure formed also confirmed the extensional regime. Fault polygon B interval is generated on the basis of all faults marked on the seismic sections to show the extensional regime. Next is to generate time and depth contour maps which also confirms the extensional regime and from the contours it can be seen that well can be drilled at darker color portion because wells usually drilled at elevated portion.

After that structural interpretation seismic attributes are applied to confirm the structural interpretation. Three seismic attributes trace envelope, instantaneous frequency and instantaneous phase are applied on line section P2094-223 by using IHS kingdom and results are shown in Figures 4.1, 4.2, and 4.3.

## References

- Ahmad, N., Fink, P., Sturrock, S., Mahmood, T., and Ibrahim, M. (2004). Sequence stratigraphy as predictive tool in Lower Goru Fairway, Lower and Middle Indus Platform, Pakistan. PAPG, ATC.
- Almutlaq, M. H., & Margrave, G. F. Tutorial: AVO inversion.
- Amigun, J.O., & Odole, O. A. (2013). Petrophysical Properties Evaluation for Reservoir Characterisation of SEYI Oil Field (Niger-Delta). *International Journal of Innovation and Applied Studies*, 3(3), 765-773.
- Asquith, G. B., Krygowski, D., and Gibson, C. R. (2004). Basic well log analysis (p. 39). American Association of Petroleum Geologists.
- Avseth, P., Mukerji, T., Mavko, G., & Dvorkin, J. (2010). Rock-physics diagnostics of depositional texture, diagenetic alterations, and reservoir heterogeneity in high-porosity siliciclastic sediments and rocks—A review of selected models and suggested work flows. *Geophysics*, 75(5), 75A31-75A47.
- Badley, M. E. (1985). Practical seismic interpretation.
- Bender. (1995). Geology of Pakistan. Berlin: Gerbruder Borntraeger.
- Castagna, J. P., & Backus, M. M. (1993). AVO analysis-tutorial and review. *Offset-dependent reflectivity: theory and practice of AVO analysis*, 3-36.
- Chopra, Satinder, and Kurt J. Marfurt. "Seismic attributes, A historical perspective." *Geophysics* 70.5 (2005): 3SO-28SO.
- Coffeen, J.A., 1986, *Seismic Exploration Fundamentals*, PennWell Publishing Co.408.
- Coulombe, C. A., Stewart, R. R., and Jones, M. J. (1993). Amplitude-versus-offset analysis using the vertical seismic profile.
- Dewar, J., & Pickford, S. (2001). Rock physics for the rest of us-an informal discussion. *CSEG Recorder*, 43-49.
- Djebbar, T. I. A. B., & Donaldson, E. C. (2004). Petrophysics.
- Dobrin, M. B., & Savit, C. H. (1988). Introduction to geophysical prospecting. *Essentials of Geology*, 3rd Edition, Stephen Marshak.
- Eskola, Pentti Eelis, 1920: "The mineral facies of rocks".

- Gadallah, M. R., & Fisher, R. (2009). Seismic Interpretation. In *Exploration Geophysics* (pp. 149-221). Springer Berlin Heidelberg.
- Ivanov, J., Miller, R. D., Lacombe, P., Johnson, C. D., and Lane Jr, J. W. (2006). Delineating a shallow fault zone and dipping bedrock strata using multichannel analysis of surface waves with a land streamer. *Geophysics*, 71(5), A39-A42.
- Kadri, I. B. (1995). *Petroleum geology of Pakistan*. Karachi: Pakistan Petroleum Limited.
- Kazmi, A.H. & Jan, M.Q. (1997) "Geology and Tectonic of Pakistan" Graphic Publishers, Karachi, Pakistan.
- Kearey, P., Brooks, M., and Hill, I. (2009). *An introduction to geophysical exploration*. John Wiley & Sons.
- Lucia, F. J., 1995, *Carbonate reservoir characterization*: New York, Springer-Verlag, 226 p.
- McQuillin, R., Bacon, M., and Barcaly, W., 1984 *An introduction to seismic interpretation*, Graham & Trotman Limited Sterling House, 66 Wilton Road London SW1V 1DE.
- Parrish, J. T., & Peterson, F. (1988). Wind directions predicted from global circulation models and wind directions determined from eolian sandstones of the western United States—A comparison. *Sedimentary Geology*, 56(1), 261-282.
- Raza, H. A., & Ahmed, R. (1990). Hydrocarbon potential of Pakistan. *Journal of Canada Pakistan Cooperation*, 4(1), 9-27.
- Reading, H. G. (1996). *Sedimentary Environments and Facies*. Blackwell Scientific Publications.
- Richardson, A. A. M. (2013). Well Correlation and Petrophysical Analysis, a Case Study of "Rickie" Field Onshore Niger Delta. *The Inter. Jour. of Engi. And Scie*, 2(12), 4-99.
- Schlumberger. (1974). *Log Interpretation Volume I Principles*. Schlumberger, New York London. p. 113.
- Sheriff, R. E., and Geldart, L. P. (1995). *Exploration Seismology*. 2nd Edition. Cambridge University Press.
- Sroor, M. (2010). *Geology & Geophysics in Oil Exploration* (p. 33).
- Stanley, Steven M. (1999). *Earth System History*. New York: W.H. Freeman and Company. p. 134.
- Staton, H. G. (1996). *Reading, Sedimentary environments and facies*. Blackwells Scientific.

- Stewart, S. A. (2012). Interpretation validation on vertically exaggerated reflection seismic sections. *Journal of Structural Geology*.
- Stoneley, R., (1995). Introduction to petroleum exploration for non geologists (p. 199). Oxford, UK: Oxford University Press.
- Subrahmanyam, D., & Rao, P. H. (2008). Seismic attributes—A review. In 7th
- Taner, M. T. (1994). Seismic attributes revisited M. Turhan Taner\*, Seismic Research Corporation, James S. Schuelke, Mobil Oil Corporation, Ronen O'Doherty, Seismic Research Corporation, and Edip Baysal.
- Tran, H. The Consortium for Research in Elastic Wave Exploration Seismology Avseth, P., Dræge, A., van Wijngaarden, A. J., Johansen, T. A., & Jørstad, A. (2008). Shale rock physics and implications for AVO analysis: A North Sea demonstration. *The Leading Edge*, 27(6), 788-797.
- White, J. E. (1983). *Underground sound: Application of seismic waves* (Vol. 253). Amsterdam: Elsevier.
- Zaigham, N. A., & Mallick, K. A. (2000). Bela ophiolite zone of southern Pakistan: Tectonic setting and associated mineral deposits. *Geological Society of America Bulletin*, 112(3), 478-489.